UNIVERSIDAD DE CHILE

FACULTAD DE CIENCIAS FÍSICAS Y MATEMÁTICAS

DEPARTAMENTO DE GEOLOGÍA

CONTRASTING RECORDS FROM MANTLE TO SURFACE OF HOLOCENE LAVAS OF TWO NEARBY ARC VOLCANIC COMPLEXES: CABURGUA-HUELEMOLLE SMALL ERUPTIVE CENTERS AND VILLARRICA VOLCANO, SOUTHERN CHILE

TESIS PARA OPTAR AL GRADO DE MAGÍSTER EN CIENCIAS, MENCIÓN GEOLOGÍA

MEMORIA PARA OPTAR AL TÍTULO DE GEÓLOGO

EDUARDO ESTEBAN MORGADO BRAVO

PROFESOR GUÍA

MIGUEL ÁNGEL PARADA REYES

MIEMBROS DE LA COMISIÓN

FRANCISCO GUTIÉRREZ FERRER

ANGELO CASTRUCCIO ÁLVAREZ

SANTIAGO DE CHILE

2015

"Contrasting records from mantle to surface of Holocene lavas of two nearby arc volcanic complexes: Caburgua-Huelemolle Small Eruptive Centers and Villarrica Volcano, Southern Chile"

La mayor parte de los centros eruptivos menores de los Andes del sur están ubicados sobre la Zona de Falla Liquiñe-Ofqui (ZFLO), una estructura mayor (>1000 km de extensión) de rumbo NS, y cercanos a volcanes mayores: los estratovolcanes. Sin embargo, las relaciones genéticas entre estos dos tipos de volcanismo es, todavía, pobremente conocido. Esta contribución compara parámetros composicionales y condiciones de presión y temperatura pre- y syn-eruptivas entre las lavas basálticas de los Centros Eruptivos Menores Caburgua-Huelemolle (CEMCH) y la lava andesita-basáltica de la erupción de 1971 del Volcán Villarrica, ubicado a 10 km de los CEMCH.

Olivinos y clinopiroxenos se encuentran como fenocristales y formando parte de cúmulos cristalinos de las lavas estudiadas. No muestran marcadas diferencias composicionales, excepto por la composición más dispersa de los clinopiroxenos. Los fenocristales de olivino comúnmente tienen inclusiones de Cr-espinelas. Los fenocristales de plagioclasas se encuentran como fenocristales de 0.7 a 2.0 mm de largo o como microlitos en una matriz sin vidrio. Dos grupos de fenocristales de plagioclasa se identificaron en la lava de 1971 basados en el tamaño de los cristales, texturas de desequilibrio y patrones de zonación. Los microlitos de plagioclasa ocupan ~ 85 % del volumen de la masa fundamental.

Las temperaturas pre-eruptivas del reservorio tipo CEMCH está entre 1162 y 1165 ± 6 °C y a presiones entre 7.7 y 14.4 kbar, lo que implica la existencia de un reservorio profundo, fueron obtenidas por geotermobarometría en olivino-clinopiroxeno. Probablemente el reservorio se ubica en el límite corteza manto (10 kbar). Además se obtuvieron escalas de tiempo a partir de los patrones de zonación de los cristales de olivino a partir de condiciones inferidas de un reservorio usando MELTS. Las mínimas escalas de tiempo van entre 11.3 y 78 días y solamente pueden ser explicadas por la presencia de al menos un reservorio en la corteza superior, de otro modo el magma en ascenso se solidificaría antes de llegar a la superficie. Los máximos intervalos de tiempo de la formación de la zonación de los cristales de olivino es de 121 días, lo que representaría el máximo tiempo de residencia en el reservorio de la corteza inferior.

Por otro lado, los fenocristales de la lava de 1971 del Volcán Villarrica tienen registros de dos etapas o pausas en el ascenso de magma hasta la superficie: 1,208 ±6 °C y 4.6 - 9.8 kbar (reservorio profundo) y 1,168 - 1,175 ±6 °C y ≤ 0.54 kbar (reservorio de poca profundidad). En este último, un calentamiento previo a la erupción de 1971 del Villarrica es grabado en los bordes más anortítitcos de los fenocristales de plagioclasa.

Los tiempos de residencia de los CEMCH, de máximo 121 días, son mucho más cortos que aquellos calculados para el Volcán Villarrica, que sería del orden de décadas. La presencia de la ZFLO bajo los centros eruptivos menores facilitaría el ascenso de magmas y disminuiría el tiempo de residencia de los magmas en la corteza.

"El fútbol es el primer deporte del mundo, es el deporte más atractivo para todos los continentes. Si yo tuviera que decir por qué sucede eso, es porque no siempre ganan los poderosos"

"Un hombre con ideas nuevas es un loco, hasta que sus ideas triunfan"

-Marcelo Alberto Bielsa Caldera, *el loco*

Agradecimientos

En primer lugar quiero agradecer a quienes siempre estuvieron conmigo acompañándome y me dieron su cariño de forma íntegra, entre bromas y comentarios de apoyo: mi familia. Mis padres, Eduardo y Liliana; mis hermanos, Loreto y Benjamín; también a Inti y Alicia, cuya presencia en nuestro hogar ha sido muy valiosa. Así mismo a mis tíos y primos, que siempre confiaron en mí incondicionalmente.

Además, me gustaría agradecer al proyecto CONICYT-FONDAP 15090013, Centro de Excelencia en Geotermia de los Andes (CEGA) por financiar los terrenos, diversos análisis que fueron necesarios para la elaboración de esta tesis y los congresos en que participé.

Quisiera agradecer a aquellas personas con quienes formamos un grupo de trabajo, ellos fueron fundamentales para cumplir con las metas que me propuse al inicio de esta tesis, de todos ellos aprendí mucho y deseo que ellos también hayan aprendido un poco, al menos, conmigo. En primer lugar a mi mentor, el profesor Miguel Ángel Parada, quien fue mi guía y consejero en diversas temáticas, desde el rigor que implica el trabajo y la forma de escribir un artículo científico hasta el ámbito personal. Al profesor (y mentor) Francisco Gutiérrez, quien siempre creyó en mis ideas y me exigió más de lo que, incluso yo, pensé que podía dar. Al profesor Angelo Castruccio, quien siempre mostró interés y confianza tanto en el trabajo que realizaba como en mis capacidades. A Lucy McGee, quien siempre tuvo paciencia para hacerme correcciones y cuyas discusiones fueron un aporte inmenso a esta tesis. A Nicolas Vinet, cuyas buenas vibras, recomendaciones de publicaciones y otras conversaciones fueron una motivación para terminar este proceso de la mejor manera. Finalmente, a Claudio Contreras, mi amigo de tantos viajes, carretes y conversaciones; en quien muchas veces me afirmé cuando lo necesitaba, pero también fue crítico cuando tuvo que serlo.

A mis amigos (casi) desde que tengo uso de razón: los Valle Hardcore (*cote*, *rolo*, *mono*, *gute*, *gurufa*, *kato*, *isa*, *klauz*, *moni*, *benja*, *carla*, *camus*, *huevo*, *silence*, *maui*, *coni* y tantos otros que han sido parte de esta segunda familia). A mis amigos de universidad, tanto de posgrado como de pregrado (seguramente estoy olvidando a muchos): *shorty (Sánchez-Bozo)*, Boyce, Ítalo (el gran máster), *angelito*, Danilo, Piero, Raúl, *feña*, *lalu*, *mumo*, *ore*, *feñi*, *flo*, *caro* Geoffroy, *mari*, Leo Navarro, Rayén, *estrella*, *coni* Nicolau, Alida, *monse*, Pablo M., Pablo S., *óscarsk8fire*, *vladi*, Tapia, Tomás I., *vale*, *nelsiton*, *diegol*.

A los profesores de los Departamentos de Geología y Geofísica de la Universidad de Chile, de quienes solamente tuve comentarios de apoyo, sobre todo a quienes me inspiraron a considerar la academia como una opción de vida (aparte de los profesores mencionados anteriormente): Martin Reich, Mario Vergara, Diego Morata, Roberto Rondanelli y especialmente a Don Luis Aguirre, cuya estimulante dedicación y caballerosidad siempre fueron más allá de la sala de clases. También a los funcionarios del Departamento de Geología de la Universidad de Chile, en particular a Blanca, Maritza y Rosita (que me salvaron más de alguna vez y siempre tuvieron una sonrisa), Bernardette, Don Carlos, Sofía, *juanito*, Quilo y especialmente a Roberto y a los Julios (padre e hijo).

Finalmente, me gustaría agradecer a todos quienes fueron mis auxiliares o alumnos en algún laboratorio a lo largo de esta larga carrera. Ellos fueron esenciales en los conocimientos que adquirí, espero también haber formado parte importante de su formación.

Tabla de contenido

Índice de figuras

Índice de tablas

CAPÍTULO 1

INTRODUCCIÓN

1.1 Estructura de la tesis

El presente trabajo se centró en el estudio de muestras de lavas de los centros eruptivos menores Caburgua-Huelemolle y la lava de la erupción de 1971 del volcán Villarrica. Se hizo particular énfasis en la mineralogía y las asociaciones mineralógicas en equilibrio para determinar reservorios para ambos complejos volcánicos.

Los **capítulos 2 y 3** corresponden a manuscritos de artículos. El capítulo 2 ya fue sometido a la revista *Journal of Volcanology and Geothermal Research*, mientras que el **capítulo 3** necesita más datos antes de ser sometido. Como se espera que ambas publicaciones sean independientes, es común encontrar que el **capítulo 3** hace referencia a datos del **capítulo 2**.

1.2 Motivación

El volcán Villarrica es uno de los centros eruptivos más activos de la Zona Volcánica Sur de los Andes, en Chile. Su altura es de 2828 m.s.n.m., con un volumen estimado de 250 km^3 que cubre un área de 400 km^2. Está ubicado en el extremo occidental de la cadena NW-SE que incluye los volcanes: Lanín, Quetrupillán y Villarrica. A una distancia de 10 kilómetros del volcán Villarrica se encuentran los centros eruptivos menores Caburgua-Huelemolle, que corresponden a centros de áreas y volúmenes mucho menores a los del Volcán

Villarrica. Además existen diferencias composicionales entre los productos de ambos centros eruptivos, Hickey-Vargas et al. (1989) proponen dos modelos para explicar esto: (1) las diferencias se deben a diferentes tasas de fusión parcial por diferencias en el aporte de fluidos, (2) diferencias en la contaminación por fundidos en el manto litosférico. Sin embargo, las condiciones de los reservorios, contaminación y ascenso de magmas en la corteza no han sido considerados en la explicación de las diferencias composicionales. Por lo tanto, los objetivos de este trabajo tienen como finalidad responder a las siguientes preguntas:

¿Qué características bajo la superficie diferencian a estos dos centros eruptivos?, ¿Por qué, en líneas generales, las lavas de los centros eruptivos menores Caburgua-Huelemolle tienen una composición más primitiva que los del volcán Villarrica?, ¿Comparten un reservorio común?

1.3 Objetivos

1.3.1 Hipótesis de trabajo

Dos complejos volcánicos cercanos con diferencias composicionales en los productos tienen diferencias en sus mecanismos de ascenso y almacenamiento bajo la superficie, estas diferencias determinan la composición y las texturas que se reconocen.

1.3.2 Objetivo general

Determinar las condiciones y procesos pre-eruptivos registrados por las lavas de los complejos volcánicos estudiados.

1.3.3 Objetivos específicos

- Caracterizar la mineralogía de las lavas, reconocer las texturas y las asociaciones minerales.

- Obtener resultados de termometría y barometría en las asociaciones minerales que lo permitan.

- Desarrollar un modelo de reservorios de la zona, que ligue los datos de termobarometría con las texturas observadas en los minerales.

- Calcular tiempos de residencia de los magmas en la corteza superior, de manera de ligarlos a los datos de termobarometría y la importancia de la fuente de calor de la zona.

- Describir los procesos pre-eruptivos para cada complejo volcánico estudiado.

CAPÍTULO 2

CONTRASTING RECORDS FROM MANTLE TO SURFACE OF HOLOCENE LAVAS OF TWO NEARBY ARC VOLCANIC COMPLEXES: CABURGUA- HUELEMOLLE SMALL ERUPTIVE CENTERS AND VILLARRICA VOLCANO, SOUTHERN CHILE

Morgado, E.[1]*, Parada, M.A.[1], Contreras, C.[1], Castruccio, A.[1], Gutiérrez, F.[1, 2], McGee, L.E. [1]

[1] Departamento de Geología, Facultad de Ciencias Físicas y Matemáticas, Universidad de Chile, Chile/ Centro de Excelencia en Geotermia de los Andes (CEGA)

[2] Advanced Mining Technology Center, Universidad de Chile

* Corresponding author at: Centro de Excelencia de Geotermia de los Andes (CEGA), Departamento de Geología, Facultad de Ciencias Físicas y Matemáticas, Universidad de Chile, Santiago 8370450, Chile.

E-mail addresses: emorgado@ing.uchile.cl (E.Morgado), maparada@cec.uchile.cl (M. Parada), clcontre@ug.uchile.cl (C.Contreras), frgutier@ing.uchile.cl (F. Gutiérrez), acastruc@ing.uchile.cl (A. Castruccio), lucymcgee@ing.uchile.cl (L. McGee).

Abstract

Most of the small eruptive centers of the Andean Southern Volcanic Zone are built over the Liquiñe-Ofqui Fault Zone (LOFZ), a NS strike-slip (> 1,000 km length) major structure, and close to large stratovolcanoes. However the genetic relationship between these two styles of volcanism is poorly known. This contribution compares textural features, compositional parameters, and pre- and

syn-eruptive P, T conditions, between basaltic lavas of the Caburgua-Huelemolle Small Eruptive Centers (CHSEC) and the 1971 basaltic andesite lava of the Villarrica Volcano located 10 km south of the CHSEC. Olivines and clinopyroxenes occur as phenocrysts and forming part of crystal clots of the studied lavas. They do not markedly show compositional differences, except for the more scattered composition of the CHSEC clinopyroxenes. Olivine phenocrysts commonly have Cr-spinels inclusions in all the studied samples. Plagioclase in CHSEC lavas mainly occur as phenocrysts of 0.7-2.0 mm long or as microlites in a glass-free matrix. Two groups of plagioclase phenocrysts were identified in the 1971 Villarrica lava based on crystal size, disequilibrium features and zonation patterns. Microlites of 1971 Villarrica samples occupy ~ 85 vol% of the glass free matrix. The presence of negative Eu-anomaly in the 1971 Villarrica REE patterns makes a difference with respect to the absence of this anomaly in the CHSEC REE patterns. Most of the CHSEC samples exhibit higher La_N/Yb_N and more scattered Sr-Nd values than 1971 Villarrica lava samples, which are clustered at higher [143]Nd/[144]Nd values. Pre-eruptive temperatures of the CHSEC-type reservoir between 1,162 and 1,165 ± 6 °C and pressures between 7.8 and 14.4 kbar consistent with a deep-seated reservoir at the mantle-crust boundary were obtained from olivine-augite phenocrysts. Conversely, olivine-augite phenocrysts of 1971 Villarrica lava samples record pre-eruptive conditions of two stages or pauses in the magma ascent to the surface: 1,208 ±6 °C and 4.6 - 9.8 kbar (deep-seated reservoir) and 1,164 - 1,175 ±6 °C and ≤ 0.54 kbar (shallow reservoir). At shallow reservoir conditions a magma heating prior to the 1971 Villarrica eruption is recorded in the more anorthitic rims of plagioclase phenocrysts. Syn-eruptive temperatures of 1,081 and 1,133 ± 6 ºC and

1,123 and 1,148 ± 6 °C were obtained in CHSEC and 1971 Villarrica lava, respectively using equilibrium olivine-augite microlite pairs. The LOFZ could facilitate a direct transport to the surface of the CHSEC magmas and explain the observed differences with the pre-eruptive conditions of the 1971 Villarrica lava.

2.1 Introduction

Small eruptive centers are present in different tectonic settings and are associated with products of different compositions, although they commonly are basaltic (Valentine and Greg, 2008; Németh, 2010; McGee et al., 2011). For example, the Jeju Island Quaternary intraplate volcanic field in Korea, is composed of alkali and sub-alkali basaltic monogenetic centers clustered on a few kilometers scale (Park et al., 1999) that were derived from a heterogeneous mantle source and independent reservoirs (Brenna et al., 2012). In the western Mexican trans-arc, the Tequila volcanic field has a bimodal composition probably caused by the emplacement of basalts that trigger partial melting of upper crustal rocks (Lewis-Kenedi et al., 2005). Many field of small eruptive centers consist of aligned volcanic cones clustered along regional structures (e.g. López-Escobar et al., 1995a; Condit and Connor, 1996; Connor et al., 1992, 2000; Conway et al., 1998; Valentine et al., 2006) and they commonly were formed by short-lived multiple eruption phases, although some of them lasted several years (e.g. Houghton and Schmincke, 1989; Brand and White, 2007).

Many attempts to explain the reasons why small eruptive centers and polygenetic volcanism can co-exist have been focused on explanations considering structural

aspects and magmatic rates. For example, crack interaction theory indicates that both high regional differential stress and low magma supply rate allow the development of small volcano fields because they prevent crack coalescence, which generate large polygenetic volcanoes (Takada, 1994a). The coexistence of small eruptive centers and large stratovolcanoes could also result from contrasting rates of magma production and/or stress regime (Takada, 1994b). Conversely, Cañón-Tapia and Walker (2004) suggest that the most important controlling factor for the small eruptive center formation with respect to stratovolcanoes is not the magma production rate, but the degree of melt interconnection through coalescing conduits where the magma ascends. Pinel and Jaupart (2000) proposed that for a given edifice dimension and overburden conditions, there is a critical magma density threshold over which the magma cannot reach the surface. These stalled magmas could evacuate by horizontally propagating dykes and then generate eruptive centers at increasing distances from the initial reservoir (Pinel and Jaupart, 2004). This model implies the existence of a common reservoir for stratovolcanoes and SECs in the upper crust.

According to some authors (e.g. Lara et al., 2006a; Cembrano and Lara, 2009) small eruptive centers of the Chilean Southern Andes are the most primitive volcanoes of the Southern Volcanic Zone (SVZ; Hildreth and Moorbath, 1988) and are commonly built over of the dextral strike-slip Liquiñe-Ofqui Fault Zone (LOFZ) and close to large stratovolcanoes (Cembrano and Lara, 2009). However, $15 - 11$ ky basalts of ≤ 49 wt % SiO_2 and ≥ 16 wt % MgO have been reported by Singer et al.

(2008) among rhyodacitic and rhyolitic lavas in Puyehue stratovolcano, these are more primitive than those from monogenetic Carrán-Los Venados basalts.

Regional structural studies conclude that some Andean SECs are spatially associated with NE-SW tension fractures, along which a rapid magma ascent is facilitated (e.g. López-Escobar et al., 1995a; Lara et al., 2006a; Cembrano and Lara, 2009). López-Escobar et al. (1995a) compared features of lavas from Osorno and Calbuco (41° - 42° S) stratovolcanoes and the nearby SECs and concluded that SECs basalts were produced as a result of lower melting degree than Osorno basalts and that Calbuco lavas have experienced more crustal assimilation than the SECs. On the other hand, Puyehue-Cordón Caulle volcanic complex (40°30'S) and the spatially associated monogenetic Carrán-Los Venados cones have similar asthenospheric sources (Lara et al., 2006a; 2006b), but they interpreted different ascent pathways: Puyehue-Cordón Caulle erupted evolved lavas, consistent with long magma residence times in the upper crust; whereas Carrán-Los Venados cones erupted more primitive volcanic materials, consistent with upwelling along regional tension cracks (Lara et al., 2006a).

This study focuses on lavas of the Caburgua-Huelemolle Small Eruptive Centers (CHSEC) and on the 1971 lava of the Villarrica Volcano. The latter lava was selected because it corresponds to a large and the best preserved Holocene lava of the Villarrica Volcano. CHSEC are composed of 20 pyroclastic cones with associated lava flows of basaltic composition that are assembled into 8 volcanic centers: Caburgua, Huelemolle, La Barda, Relicura, Cañi, Redondo, Cordillera Cañi and San Jorge (Fig. 2.1). Four lavas from the each cone of Caburgua, three lavas from each

cone of Huelemolle, one lava from the San Jorge cone and 5 samples from the 1971 Villarrica lava were selected to study the pre-eruptive conditions from the magma reservoirs up to the surface using whole-rock geochemistry, mineral chemistry, and thermobarometric tools. Particular emphasis is placed on the existence of deep reservoirs in both volcanic complexes and on the independent paths of the ascending magma to the surface. Previous studies have been focused on the geochemical and isotopic characteristics to constrain the nature of the magma source (Hickey-Vargas et al., 1989; 2002) and have concluded that differences between Villarrica volcano and CHSEC could be explained by independent origins from heterogeneous sources, probably associated to variable effects of slab-derived fluids. Differences in major and trace elements and isotopic ratios have been observed between San Jorge cone and the rest of the CHSEC of the zone. However, they are very similar to those obtained in the Villarrica 1971 eruption, suggesting a geochemical connection between Villarrica volcano and at least one of the CHSEC (Hickey-Vargas et al., 2002).

2.1.1 Caburgua-Huelemolle Small Eruptive Centers (CHSEC)

CHSEC are located at the south of Caburgua Lake (Fig. 2.1), 10 km north of Villarrica Volcano. Some of the small eruptive centers correspond to volcanic cone clusters: Caburgua (four cones), Huelemolle (three cones), La Barda (three cones), Relicura (five cones), and Cordillera Cañi (two cones). Cañi, Redondo and San Jorge are volcanic centers formed by a single cone (Fig. 2.1). Two directions of cone alignments are recognized (Fig. 2.1): NNE that coincides with the dextral Liquiñe-Ofqui Fault (LOFZ) and NE that coincides with tension cracks (duplex) of the LOFZ

(Cembrano et al., 1996; Cembrano and Lara, 2009). The main characteristics of CHSEC cones are provided in Table 2.1.

The CHSEC lavas are basalts (49-52 wt %; Table 2.2) that contain plagioclase, olivine and clinopyroxene pheonocrysts with glomeroporphiric, traquitic and intergranular textures. Most of the CHSEC lavas are phenocryst-poor (3-10 vol %), with the exception of the San Jorge lava, which has phenocryst content of 13-18 vol %. The percentage of vesicles in CHSEC varies between 4 and 14 vol.%.

The age of the Huelemolle volcanic activity weas estimated as at least 9,000 years old by a ^{14}C dating of carbonized wood collected into pyroclastic deposits (Moreno and Clavero, 2006). The ages for the other small eruptive centers are not well-constrained but the absence of glacial erosion suggests being post-glacial Holocene.

2.1.2 Summary of Villarrica Volcano and its 1971 eruption

Villarrica Volcano is one of the most active volcanic centers of the Southern Andean Volcanic Zone. Its height is 2,828 m.a.s.l., with an estimated volume of 250 km^3 that covers an area of 400 km^2. It is located at the westernmost position of the NW-SE volcanic chain that also includes Quetrupillán and Lanín stratovolcanoes (López-Escobar et al., 1995b; Stern et al., 2007). Villarrica Volcano, which started its activity at least 600 ky. ago (Moreno and Clavero, 2006) and has produced basalts and basaltic andesite lava flows and pyroclastic deposits, which are divided into three units (Clavero and Moreno, 2004; Moreno and Clavero, 2006): Villarrica I (Middle to Upper Pleistocene), Villarrica II (Holocene, between 13.9 and 3.7 ky) and Villarrica III (< 3.7 ky). Unit Villarrica III has a historical record of eruptions; some of them correspond to lavas of the following eruptions: 1787, 1921, 1948,

1963, 1964, 1971 and 1984. Currently, the volcano is characterized by a lava lake and constant degassing and seismicity (Calder et al., 2004). The 1971 Villarrica eruption generated two Aa-type lavas. The eruption began in October with strombolian explosions and lava effusions along the Challupén Valley (SW flank). In November, two pyroclastic cones grew inside the crater simultaneously with lava effusion. During the night of the December 30th, the eruption reached its paroxysmal phase, with a lava fountain > 500 m high and effusion rates ~ 500 m^3/s, generating two lava flows of 6 and 16.5 km that flowed along the Pedregoso and Challupén valleys, respectively and were emplaced in less than 48 hours. The total erupted volume is ~ 0.03 km^3 (Moreno, 1993; Moreno and Clavero, 2006 and references therein). The studied lava has phenocrysts (14-17 vol %) of plagioclase, olivine and clinopyroxenes, and vesicles that reach up to 13 vol %. The most common textures are glomeroporphiric, traquitic, poikilitic, ophitic and subophitic.

2.2 Analytical Procedure

Sixteen samples from CHSEC lavas and five from the 1971 Villarrica lava were studied for geochemical, isotopic and mineralogical analysis. The CHSEC samples were collected from three *Pahoehoe* lavas of Caburgua, three Aa lavas of Huelemolle, and one of each *Aa* lava of San Jorge, La Barda, Relicura, Cañi, Redondo and Cordillera Cañi. Five samples were collected along the 1971 Villarrica lava. Whole-rock compositions were analysed by XRF (major elements) and ICP-MS (trace elements) at ACT-Labs using BIR-1a, DNC-1, W-2a and DNC-1 standards. The precision was < 9% 2σ and accuracy was mostly better than 3%. The Sr and Nd isotope data were obtained for 8 samples (one sample for each

CHSEC) with a Triton multi-collector mass-spectometer at ACT-Labs using the standards JNd-1 (for Nd isotopes) and NBS 987 (for Sr isotopes). The mineralogical studies were carried out with a Scanning Electron Microscope (SEM) at the University of Chile (FEI Quanta 250) and electron microprobe at the School of Geosciences, University of Edinburgh (Cameca SX100; nine samples) and at LAMARX- National University of Cordoba (JEOL JXA-8230; six samples). The analytical conditions for the eight CHSEC samples analyzed by the Cameca SX100 consisted of an accelerating potential of 15 kV and electron beam current of 4 nA for major elements and 100 nA for minor and trace elements. Counting times for major elements were 20 seconds on peak and 10 seconds on background. The mineral composition of the two samples from CHSEC and four from 1971 Villarrica lava measured by the JEOL JXA 8230 were obtained with an accelerating potential of 15 kV and electron beam current of 20 nA (10 nA for plagioclase). Counting times were 10 seconds for peak and 5 seconds at each background position for major and minor elements.

2.3 Geochemical and isotopic data

The analyzed CHSEC lavas are basalts (49.37-51.77%) and have lower SiO_2 contents than the 1971 Villarrica basaltic-andesite samples (51.76-52.93%) (Fig 2.2a). All the CHSEC and Villarrica samples correspond to the calcalkaline series, except for San Jorge samples, which have tholeiitic affinities (Fig. 2.2b). The CHSEC have Mg# values between 0.48 and 0.69, whereas 1971 Villarrica samples have Mg# values between 0.56 and 0.59. For a given MgO composition, the CHSEC basalts have

higher Al_2O_3, K_2O and P_2O_5 and lower Ni, Cr, Sc, V contents than Villarrica samples (Hickey-Vargas et al., 1989). Most CHSEC samples have similar trace element contents (Fig. 2.3) and La_N/Yb_N (8.47-10.5). The exceptions are the San Jorge samples, which have lower trace element contents and La_N/Yb_N (4-4.33). Villarrica shows a La_N/Yb_N ratio between 2.88 and 3.73. All the samples display Nb-Ta anomalies (Fig. 2.3a). CHSEC do not have Eu anomalies, but all Villarrica samples have small Eu anomalies (Fig 2.3b). Most CHSEC samples have Dy_N/Yb_N (cf. Davidson et al., 2013) values between 1.79 and 2.0. The exceptions are the San Jorge samples, which have Dy_N/Yb_N values between 1.6 and 1.7, similar to those values of the 1971 Villarrica lava samples (1.54 and 1.77).

Available and new data of Sr and Nd ratios of CHSEC and Villarrica are listed in Table 2.3 and plotted in Fig. 2.4. CHSEC samples have [87]Sr/[86]Sr ratios in the range from 0.703762 ± 4 (Caburgua) to 0.704028 (San Jorge), whereas the [87]Sr/[86]Sr ratios of the Villarrica samples are higher but within a narrower range from 0.70398 ± 3 (Unit Villarrica III) to 0.70410 ± 3 (Unit Villarrica I) (Hickey-Vargas et al., 1989). [143]Nd/[144]Nd ratios of the CHSEC samples range from 0.512801 ± 2 (C. Cañi) to 0.512913 ± 4 (San Jorge), the Villarrica samples range from 0.512866 ± 22 (Unit Villarrica I) to 0.512903 ± 3 (Unit Villarrica III) (Hickey-Vargas et al., 1989). San Jorge and Cañi cones have similar Sr-Nd isotopic values to those of Villarrica volcano and differ from those of the remainder CHSEC samples (Fig. 2.4).

2.4 Mineral Chemistry

2.4.1 CHSEC plagioclases

Plagioclase phenocrysts are 0.7-2.0 mm in size and some of them have disequilibrium features in the form of patch and sieve textures. Plagioclase crystals of similar size also occur as clots with olivine, but unlike phenocrysts they do not exhibit disequilibrium features. The core compositions of plagioclase phenocrysts are fairly constant of An_{73-80} (Fig. 2.5a) and are similar in composition to the core plagioclase-forming clots. A thin rim (< 40 μm) An_{45-65} is commonly found in plagioclase phenocrysts as well as in plagioclase-forming clots, but in the latter case only around crystal faces in contact with the matrix. CHSEC lavas have glass-free matrices with abundant microlites commonly forming part of a traquitic or intergranular textures. The plagioclase microlite compositions are An_{45-58} (Fig. 2.5b). Some plagioclase microlites are hosted in plagioclase phenocryst rims indicating that, at least a portion of those rims grew coevally with microlites.

2.4.2 CHSEC mafic minerals and spinels

In CHSEC samples the olivine phenocrysts occur as isolated crystals or forming part of crystal clots together with plagioclase and commonly show disequilibrium features such as resorption and thin compositional rims. The core compositions of olivine phenocrysts and olivine-forming clots vary between Fo_{81} and Fo_{87} (Fig. 2.6a), and exhibit thin rims with compositions that vary between Fo_{73} and Fo_{80}. As with the plagioclase-forming clots, olivine-forming clots show rims only around non-armored faces. The olivine microlites occur as intergranular grains of 40-100 μm size with compositions in the Fo_{59-77} range (Fig. 2.6b). Clinopyroxene

phenocrysts are very scarce and have compositions in the range of Wo_{44-46}, En_{45-47}, Fs_{7-9} (Fig. 2.6c). Clinopyroxene microlites occur as small crystals of 5 and 92 μm and exhibit compositions in the range of Wo_{8-40}, En_{37-63}, Fs_{13-31} (Fig. 2.6d).

Chromian-spinel inclusions are abundant in olivine phenocrysts and very scarce in plagioclase phenocrysts. They also occur as isolated crystals of 5-65 μm size or forming crystal clots. The composition of chromian-spinel inclusions are: #Cr = 25-39 and #Mg= 33-59. Titanomagnetites (Mt_{35-42}, Usp_{58-65}) were found as euhedral crystals or with skeletal features in the studied CHSEC samples except in San Jorge samples, where hematites were found. The size of the Fe-Ti oxide minerals vary between 5 and 30 micrometers.

2.4.3 1971 Villarrica lava plagioclases

The modal content of plagioclase phenocrysts represents ~12 % of the total rock volume (~60-80 vol. % of phenocrysts). Two groups of plagioclase phenocrysts were identified (Fig. 2.5c) according to crystal size and disequilibrium features. Group 1 includes 0.4-4.1 mm long phenocrysts with three zones (Fig. 2.7a): oscillatory-zoned core (An_{45-74}) normal-zoned intermediate zone (An_{38-44}) and reverse-zoned rim (An_{74-46}). The first two zones exhibit disequilibrium features in the form of patch and sieve textures. Group 2 (Fig. 2.7b) includes the smallest plagioclase phenocrysts (0.3-2.0 mm) that exhibit oscillatory-zoned cores of An_{39-49}, and thin reverse-zoned rims of An_{50-73}. These rim compositions are similar to the rim compositions of the Group 1 plagioclase phenocrysts (Fig. 2.5c). Large plagioclase crystals also occur as part of clots with olivine and scarce clinopyroxene and have compositions and sizes (An_{51-73}, 0.4 - 4.1 mm long) similar to the core of

15

Group 1 plagioclases. Microlites of 1971 Villarrica samples (< 300 µm) occupy ~ 85 vol.% of the glass free matrix and exhibit compositions of An_{48-75} (Fig. 2.5b).

2.4.4 1971 Villarrica lava mafic minerals and spinels

The modal content of the olivine phenocryst is between 2 and 4% and are found as isolated crystals (up to 4 mm long), forming clots (up to 4 mm long) or chadacrysts (~180 µm long). They have commonly resorption features and compositional rims that do not exceed 30 µm. The core compositions vary between Fo_{75} and Fo_{79} (Fig. 2.6a), and the rim composition slightly varies between Fo_{65} and Fo_{67}. The rims of olivine-forming clots are only developed around non-armored faces. The scarce olivine microlites (~ 5% of the groundmass) have sizes between 10 and 30 µm and compositions of Fo_{63-67} (Fig. 2.6b) similar to the rim phenocryst composition. Clinopyroxenes of variable composition (Wo_{37-40}, En_{47-49}, Fs_{12-13}; Fig. 2.6c) occur as isolated crystals (0.6–1.5 mm) and oikocrysts within plagioclase and olivine chadacrysts. Clinopyroxene in the matrix varies between 15 and 40 µm long with compositions of Wo_{8-17}, En_{57-65}, Fs_{25-31} (Fig. 2.6d).

Chromian-spinel are found as inclusions of 15-50 µm in olivine phenocrysts and have compositions of #Cr = 53-62 and #Mg= 26-30. Titanomagnetite crystals of 5-20 µm and compositions of (Mt_{33-44}, Usp_{56-67}) were found as euhedral isolated crystals or exhibiting skeletal features in the matrix.

2.5 Results and discussion

2.5.1 Implications of the compositional signatures of the studied lavas

All the studied samples exhibit similar arc-related geochemical signatures such as calc-alkaline affinities (Fig. 2.2b) and negative Nb-Ta anomalies (Fig. 2.3a), however the presence of negative Eu-anomaly in the 1971 Villarrica REE patterns makes a difference with respect to the absence of this anomaly in the CHSEC patterns, suggesting plagioclase as a residual phase in the Villarrica lava. Additionally, the wide range of Sr-Nd isotope ratios observed in CHSEC (Fig. 2.4), despite the proximity between centers, could indicate local-scale mantle source heterogeneities. The limited range in isotopic values of Villarrica volcano that differ from most of the CHSEC data is indicative of a homogenous mantle source despite its substantially longer history of volcanic activity (~600 ky). Differences in magma sources of CHSEC and Villarrica volcano have also been suggested by Hickey-Vargas et al. (1989).

2.5.2 Reservoirs at the mantle-crust boundary

P,T conditions

The olivine-augite geothermometer (Loucks, 1996) and olivine-clinopyroxene geothermobarometer (Köhler & Brey, 1990) were used in the same olivine-clinopyroxene pairs (isolated phenocrysts or in crystal clots) of CHSEC and 1971 Villarrica lava (Table 4). The equilibrium conditions between olivine and augite pairs were tested using Grove et al. (1997) equations (Fig. 8) to determine if both minerals are in equilibrium with the same melt composition in terms of Fe/Mg

17

values. Olivine-augite pairs of two CHSEC samples (CAB1-1 and SANJ-1) and two 1971 Villarrica lava samples (1971 10 M1 and 1971 N6) satisfied the mentioned equilibrium conditions with melts with Fe/Mg values of 0.5-0.6 (CHSEC) and 1-1.1 (Villarrica). These values are substantially different than those of the hosting sample composition, thus an antecrystic origin is inferred for these olivine and augite crystals. Equilibrium temperatures between 1,162 and 1,165 ±6 °C (Fig. 8a) and pressures between 7.8 and 14.4 kbar were obtained for the CHSEC olivine-augite antecryst pairs (Table 4). This pressure range includes the estimated pressure of ~ 10 kbar (~38 km) for the mantle-crust boundary beneath the Andes at this latitude (Folguera et al., 2007). Because the mantle-crust boundary constitutes a rheological barrier that facilitates mantle-derived magma storage (Hildreth and Moorbath, 1988) we favor CHSEC magma reservoir pressures consistent with this boundary. The absence in the CHSEC samples of thermobarometric evidence of shallow reservoirs or pauses during the magma ascent to the surface is consistent with a single-reservoir magma system. For the 1971 Villarrica lava temperatures of 1,208 ± 6°C (Fig. 8b) and pressure of 4.6-9.8 kbar were obtained from olivine-augite phenocrysts thermometry and barometry (Fig. 9c; Table 4). As with CHSEC, we favor the highest pressures for the Villarrica volcano deep reservoir.

2.5.3 Shallow reservoir of the 1971 Villarrica lava

Conditions of a shallow magma reservoir for Villarrica volcano have been provided by Lohmar et al., (2012) from a study of the ~13 ky Licán Ignimbrite (pressures of < 0.67 kbar and T of ~ 900 and ~ 1,100 °C as a consequence of heating). Shallow

reservoir conditions of the 1971 Villarrica lava were also identified using the olivine-augite thermobarometry (sample 1971 10 M1): pressures up to 2.4 kbar and associated temperatures between 1,164 and 1,175 ± 6°C were calculated in olivine-augite pairs of a single clot (Fig. 9b; Table 4).

Additionally, the shallow reservoir conditions (P, T, f_{O2} and H_2O content) were calculated using MELTS by reproducing the compositions of Group 2 plagioclase cores (An_{39-49}) and plagioclase phenocryst rims (An_{74}). The Group 2 plagioclase core compositions were obtained under equilibrium at <0.8 kbar, temperatures of 915-970° C, dissolved H_2O content of 1-3.1 wt % and NNO oxygen fugacities. Plagioclase rim compositions were also reproduced under equilibrium at similar pressures (<0.9 kbar) and oxygen fugacities (NNO), but at higher temperatures (1,120-1,180 °C) and lower dissolved H_2O content (0.3-1.2 wt %) than Group 2 plagioclase cores. By considering the plagioclase phenocryst rims as representative of the late stage of plagioclase formation at the shallow reservoir, these differences would indicate a heating and subsequent magma degassing prior to the eruption. Changes in pressure and water content associated with heating were also calculated by iteration of the empirical model equation for the solubility of water in basaltic melts (Moore et al., 1998) and the plagioclase-liquid hygrometer calibrated by Lange et al. (2009) (details in Appendix I). Using the same parameters (melt and plagioclase compositions), temperatures of 970 and 1,180 °C were used for Group 2 plagioclase core compositions and plagioclase phenocryst rim compositions, respectively. The heating of the shallow reservoir (at a calculated depth equivalent to 0.54 kbar) would be associated to a decompression of 0.4 kbar and a H_2O

exsolution of 1 wt % (Fig A1). We speculate that the heating triggers the 1971 eruption with the subsequent decompression.

2.5.4 Syn-eruptive conditions

We estimate syn-eruptive temperatures using equilibrium olivine-augite (Loucks, 1996) microlite pairs of four samples (Fig. 8) from both CHSEC (CAB1-1; CAB 1-2) and 1971 Villarrica lavas (1971 N6; 1971 10 M1). The calculated CHSEC temperature values are between 1,081 and 1,133 $\pm$ 6 °C (Fig. 8a), whereas olivine-augite microlite pairs of 1971 Villarrica lava gave values between 1,123 and 1,148 $\pm$ 6 °C (Fig. 8b).

Additionally, we reproduce by MELTS the temperature of the plagioclase microlite crystallization considering the microlite composition of the more abundant sizes: 30-60 μm (An_{59-60}) and 60-100 μm (An_{64-66}) for CHSEC and 1971 Villarrica lava, respectively. The calculated CHSEC syn-eruptive temperatures are between 1,130 and 1,137 °C at crystal content between 45 and 52 vol %. For the 1971 Villarrica eruption the calculated temperatures are between 1,150 and 1,160 °C at crystal content between 23 and 35 vol %. It is interesting to note that the 1971Villarrica lava plagioclase microlites crystallized at slightly lower temperatures than those of plagioclase phenocryst rims (1,180°C) but higher than the 970°C of the Group 2 plagioclase core crystallization, consistent with the mentioned heating as a triggering mechanism of the eruption. Despite the high crystallinity calculated for the selected CHSEC lava, the effective consistencies determined from the modified Einstein-Roscoe equation (Castruccio et al., 2010) are between 4 and 16 kPa s,

which are adequate for a basaltic lava to flow (e.g. 1984 Mauna Loa eruption; Lipman and Banks, 1987).

2.6 Conclusions

The Caburgua-Huelemolle Small Eruptive Centers (CHSEC) and Villarrica Volcano are an example of coexistence of small eruptive centers and stratovolcanoes, a feature very common in the Southern Volcanic Zone. There are similarities between CHSEC and 1971 Villarrica lavas. In both cases the lavas were fed from deep reservoirs with temperature and pressure conditions coincident with the depth of mantle-crust boundary. However, there are significant differences with respect to pre-eruptive upper crustal magma history. CHSEC magmas would have migrated directly to the surface from the deep reservoir, whereas the 1971 Villarrica lava would have had a more complex history consistent with higher rates of magma supply (relative low rates would be associated with monogenetic volcanism; Takada, 1996a) and with an intermediate reservoir at shallow depth that underwent a heating episode prior to eruption.

The active LOFZ that controls the distribution of CHSEC could facilitate a direct transport to the surface of their magmas ponded at the base of the crust, whereas the Villarrica Volcano is built over an inactive NW-SE basement fault (Moreno and Clavero, 2006). This tectonic situation, together with the overburden exerted by the Villarrica Volcano edifice, would have hindered the magma ascent (see Pinel and Jaupart, 2000) and facilitated the shallow reservoir construction.

Acknowledgments

Appendix I

We calculated the magma H_2O solubility and pressure conditions of the 1971 Villarrica shallow reservoir from a melt composition equivalent to the R1971 DV sample (Table 2.2) through an iterative combination of the following expressions provided by Moore´s et al. (1998) and Lange et al. (2009):

Moore´s et al. (1998) expression:

$$2ln^{melt}X_{H_2O} = \frac{a}{T} + \sum b_i X_i \frac{P}{T} + c\ ln^{fluid}f_{H_2O} + d \quad Eq.\,A1$$

where $^{melt}X_{H_2O}$ is the mole fraction of H_2O dissolved in the melt, T is temperature (Kelvin), P is pressure (bar), X_i is the anhydrous mole fraction of melt components, and *a*, *b*, *c* and *d* are the regression coefficients.

Lange´s et al., (2009) expression:

$$^{melt}X_{H_2O} = m'x + a' + \frac{b'}{T} + \sum d'_i X_i \quad Eq. A2$$

where x is a variable state dependent on enthalpy, entropy, volume, pressure, temperature and melt and crystallizing plagioclases compositions; m', a', b' and d'_i are regression coefficients of calibration.

This approach assumes core/rim Group 2 plagioclase phenocrysts composition (An_{49}/An_{74}) and temperatures of crystallization (970/1,180°C). The resulting pressures were 0.53 and 0.13 kbar for core and rim plagioclases crystallization, respectively. The calculated H_2O content of the melt is 1.6 and 0.6 wt %, at the core and rim plagioclase phenocryst crystallization, respectively.

References

Alaniz-Álvarez, S., Nieto-Samaniego, Á. F., Ferrari, L., 1998. Effect of strain rate in distribution of monogenetic and polygenetic volcanism in the Transmexican volcanic belt. Geology 26 (7), 591-594. http://dx.doi.org/10.1130/0091-7613(1998)026<0591:EOSRIT>2.3.CO;2

Aravena, D., Lahsen, A., 2012. Assessment of exploitable geothermal resources using magmatic heat transfer method, Maule Region, Southern Volcanic Zone, Chile. Geothermal Resources Council Transactions 36, 1307-1313.

Asimow, P.D., Ghiorso, M.S., 1998. Algorithmic modifications extending melts to calculate subsolidus phase relations. American Mineralogist 83, 1127–1131.

Brand, B.D., White, C.M., 2007. Origin and stratigraphy of phreatomagmatic deposits at the Pleitocene Sinker Butte Volcano, Western Snake River Plain, Idaho: Journal of Volcanology and Geothermal Research 160, 319-339. http://dx.doi.org/10.1016/j.jvolgeores.2006.10.007

Brenna, M., Cronin, S.J., Smith, I.E., Maas, R., Sohn, Y.K., 2012. How small-volume basaltic magmatic systems develop: a case study from the Jeju Island volcanic field, Korea. Journal of Petrology 53 (5), 985-1018. http://dx.doi.org/10.1093/petrology/egs007

Calder, E., A. Harris, P. Peña, E. Pilger, L. Flynn, G. Fuentealba, and H. Moreno, 2004. Combined thermal and seismic analysis of the Villarrica Volcano lava lake, Chile. Revista Geológica de Chile, 31(2), 259–272. http://dx.doi.org/10.4067/S0716-02082004000200005

Cañón-Tapia, E., Walker, G.P.L., 2004. Global aspects of volcanism: the perspective of "plate tectonics" and "volcanic systems". Earth-Science Reviews 66, 163-182. http://dx.doi.org/10.1016/j.earscirev.2003.11.001

Castruccio, A., Rust, A.C., Sparks, R.S.J., 2010. Rheology and flow of crystal-bearing lavas: Insights from analogue gravity currents. Earth and Planetary Science Letters 297, 471-480. http://dx.doi.org/10.1016/j.epsl.2010.06.051

Cembrano, J., Hervé, F., Lavenu, A., 1996. The Liquiñe Ofqui fault zone: a long lived intra-arc fault system in southern Chile. Tectonophysics 256, 55-66. http://dx.doi.org/10.1016/0040-1951(95)00066-6

Cembrano, J., Lara, L., 2009. The link between volcanism and tectonics in the southern volcanic zone of the Chilean Andes: A review. Tectonophysics 471, 96-113. http://dx.doi.org/10.1016/j.tecto.2009.02.038

Clavero, J., Moreno, H., 2004. Evolution of Villarrica Volcano. In: Lara, L., Clavero, J. (Eds.), Villarrica Volcano (39.5°S), Southern Andes, Chile. Boletín 61. Servicio Nacional de Geología y Minería, Santiago, 17–27.

Condit, C.D., Connor, C.B., 1996. Recurrence rates of volcanism in basaltic volcanic fields: An example from the Springerville volcanic field, Arizona. Geological Society of America Bulletin 108, 1225-1241. http://dx.doi.org/10.1130/0016-7606(1996)108<1225:RROVIB>2.3.CO;2

Connor, C.B., Condit, C.D., Crumpler, L.S., Aubele, J.C., 1992. Evidence of regional structural controls on vent distribution – Springerville Volcanic Field, Arizona. Journal of Geophysical Research 97, 12349 – 12359. http://dx.doi.org/10.1029/92JB00929

Connor, C.B., Stamatakos, J.A., Ferrill, D.A., Hill, B.E., Ofoegbu, G.I., Conway, F.M., Sagar, B., Trapp, J., 2000. Geologic factors controlling patterns of small-volume basaltic volcanism: application to a volcanic hazards assessment at Yuca Mountain, Nevada. Journal of Geophysical Research 105 (1), 417 – 432. http://dx.doi.org/10.1029/1999JB900353

Conway, F.M., Connor, C.B., Hill, B.E., Conduit, C.D., Mullaney, K., Hall, C.M., 1998. Recurrence rates of basaltic volcanism in SP Cluster, San Francisco volcanic field, Arizona. Geology 26 (7), 655 – 658. http://dx.doi.org/10.1130/0091-7613(1998)026<0655:RROBVI>2.3.CO;2

Davidson, J., Turner, S., Plank, T., 2013. Dy/Dy*: Variations arising from mantle sources and petrogenetic processes. Journal of Petrology 54, 3, 525-537. http://dx.doi.org/10.1093/petrology/egs076

Droop, G.T.R., 1987. A general equation for estimating Fe^{3+} concentrations in ferromagnesian silicates and oxides from microprobe analyses, using stoichiometric criteria. Mineralogical Magazine 51, 431–435. http://dx.doi.org/10.1180/minmag.1987.051.361.10

Foley, S.F., Prelevic, D., Rehfeldt, T., Jacob, D.E., 2013. Minor and trace elements in olivine as probes into early igneous and mantle melting processes. Earth and Planetary Science Letters 363, 181-191. http://dx.doi.org/10.1016/j.epsl.2012.11.025

Folguera, A., Introcaso, A., Giménez, M., Ruiz, F., Martínez, P., Tunstall, C., García Morabito, E., Ramos, V., 2007. Crustal attenuation in the Southern Andean retroarc (38°–39°30′ S) determined from tectonic and gravimetric studies: The Lonco-Luán asthenospheric anomaly. Tectonophysics 439, 129-147. http://dx.doi.org/10.1016/j.tecto.2007.04.001

Ghiorso, M.S., Sack, R.O., 1995. Chemical mass transfer in magmatic processes: IV. A revised and internally consistent thermodynamic model for the interpolation and extrapolation of liquid–solid equilibria in magmatic systems at elevated temperatures and pressures. Contributions to Mineralogy and Petrology 119, 197–212. http://dx.doi.org/10.1007/BF00307281

Grove, T.L., Donnelly-Nolan, J.M., Housh, T., 1997. Magmatic processes that generated the rhyolite of Glass Mountain, Medicine Lake Volcano, N. California. Contributions to Mineralogy and Petrology 127, 205–223. http://dx.doi.org/10.1007/s004100050276

Gutiérrez, F., Gioncada, A., González-Ferrán, O., Lahsen, A., Mazzuoli, R., 2005. The Hudson Volcano and surrounding monogenetic centres (Chilean Patagonia): An example of volcanism associated with ridge–trench collision environment. Journal of volcanology and geothermal research 145(3–4): 207-233. http://dx.doi.org/10.1016/j.jvolgeores.2005.01.014

Hickey-Vargas, R., Moreno, H., López Escobar, L., Frey, F., 1989. Geochemical variations in Andean basaltic and silicic lavas from the Villarrica–Lanín volcanic chain (39.5°S): an evaluation of source heterogeneity, fractional crystallization and crustal assimilation. Contributions to Mineralogy and Petrology 103, 361–386. http://dx.doi.org/10.1007/BF00402922

Hickey-Vargas, R., Sun, M., López-Escobar, L., Moreno, H., Reagan, M.K., Morris, J.D., Ryan, J.G., 2002. Multiple subduction components in the mantle wedge: evidence from eruptive centers in the Central Southern volcanic zone, Chile.

Geology 30, 199–202. http://dx.doi.org/10.1130/0091-7613(2002)030<0199:MSCITM>2.0.CO;2

Hildreth, W., Moorbath, S., 1988. Crustal contributions to arc magmatism in the Andes of Central Chile. Contributions to Mineralogy and Petrology 98 (4), p. 455-489. http://dx.doi.org/10.1007/BF00372365

Houghton, B.F., Schmincke, H.U., 1989. Rothenberg scoria cone, East Eifel: A complex strombolian and phreatomagmatic volcano. Bulletin of Volcanology 52, 28-48. http://dx.doi.org/10.1007/BF00641385

Köhler, T.P., Brey, G.P., 1990. Calcium exchange between olivine and clinopyroxene calibrated as a geothermobarometer for natural peridotites from 2 to 60 kb with applications. Geochimica et Cosmochimica Acta 54, 2375-2388. http://dx.doi.org/10.1016/0016-7037(90)90226-B

Irvine, T.N., Baragar, W.R.A., 1971. A guide to the chemical classification of the common volcanic rocks. Canadian Journal of Earth Sciences 8(5), 523-548. http://dx.doi.org/10.1139/e71-055

Lange, R.A., Frey, H.M., Hector, J., 2009. A thermodynamic model for the plagioclase-liquid hygrometer/thermometer. American Mineralogist 94, 494-506. http://dx.doi.org/10.2138/am.2009.3011

Lara, L., Lavenu, A., Cembrano, J., Rodríguez, C., 2006a. Structural controls of volcanism in transversal chains: Resheared faults and neotectonics in the Cordón Caulle–Puyehue area (40.5°S), Southern Andes. Journal of Volcanology and Geothermal Research 158, 70-86. http://dx.doi.org/10.1016/j.jvolgeores.2006.04.017

Lara, L., Moreno, H., Naranjo, J.A., Matthews, S., Pérez de Arce, C., 2006b. Magmatic evolution of the Puyehue–Cordón Caulle Volcanic Complex (40° S), Southern Andean Volcanic Zone: From shield to unusual rhyolitic fissure volcanism. Journal of Volcanology and Geothermal Research 157, 343-366. http://dx.doi.org/10.1016/j.jvolgeores.2006.04.010

Le Bas, M.J., Le Maitre, R.W., Streckeisen, A., Zanettin, B., 1986. A chemical classification of volcanic-rocks based on the Total Alkali Silica diagram. Journal of Petrology 3, 745-750. http://dx.doi.org/10.1093/petrology/27.3.745

Lewis-Kenedi, C.B., Lange, R.A., Hall, C.M., Delgado-Granado, H., 2005. The eruptive history of the Tequila volcanic field, western Mexico: ages, volumes, and relative proportions of lava types. Bulletin of Volcanology 67, 319-414. http://dx.doi.org/10.1007/s00445-004-0377-3

Lipman, P.W., Banks, N.G., 1987. Aa flow dynamics, Mauna Loa. In: Decker W., Wright, T.L., Stauffer, P.H. (Eds.), Volcanism in Hawaii. US Geological Survey Professional Paper 1350, 1527–1567.

Lohmar, S., Parada, M.A., Gutiérrez, F., Robin, C, Gerbe, M.C., 2012. Mineralogical and numerical approaches to establish the pre-eruptive conditions of the mafic Licán Ignimbrite, Villarrica Volcano (Chilean Southern Andes). Journal of Volcanology and Geothermal Research 235-236, 55-69. http://dx.doi.org/10.1016/j.jvolgeores.2012.05.006

López-Escobar , L., Parada, M.A., Hickey-Vargas, R., Frey, F.A., Kempton, P.D., Moreno, H., 1995a. Calbuco Volcano and minor eruptive centers distributed along the Liquiñe-Ofqui Fault Zone, Chile (41º-42º S): contrasting origin of andesitic and basaltic magma in the Southern Volcanic Zone of the Andes. Contributions to Mineralogy and Petrology 119, 345-36. http://dx.doi.org/10.1007/BF00286934

López-Escobar, L., Cembrano, J., Moreno, H., 1995b. Geochemistry and tectonics of the Chilean Southern Andes basaltic quaternary volcanism (37–46°S). Revista Geológica de Chile 22 (2), 219–234.

Loucks, R., 1996. A precise olivine–augite Mg–Fe-exchange geothermometer. Contributions to Mineralogy and Petrology 125, 140–150. http://dx.doi.org/10.1007/s004100050211

Marsh, B.D., 1996. Solidification fronts and magmatic evolution. Mineralogical Magazine 60, 5-40.

McGee, L.E., Beier, C., Smith, I.E.M., Turner, S., 2011. Dynamics of melting beneath a small-scale basaltic system: a U-Th–Ra study from Rangitoto Volcano, Auckland volcanic field, New Zealand. Contributions to Mineralogy and Petrology 162 (3), 547-563. http://dx.doi.org/10.1007/s00410-011-0611-x

Moore, G., Vennemann, T., Carmichael, I.S.E., 1998. An empirical model for the solubility of H_2O in magmas to 3 kilobars. American Mineralogist 83, 36-42.

Moreno, H., 1993. Volcán Villarrica. Geología y evaluación del riesgo volcánico, regiones IX y X, 39º25'S. Servicio Nacional de Geología y Minería.

Moreno, H., Clavero, J., 2006. Geología del volcán Villarrica, Regiones de La Araucanía y de Los Lagos. Servicio Nacional de Geología y Minería, Carta Geológica de Chile, erie Geología Básica, No. 98, Mapa escala 1:50000.

Moreno, H., Lara, L., 2008. Geología del área Pucón-Curarrehue, regiones de La Araucania y De Los Ríos. Servicio Nacional de Geología y Minería, Carta Geológica de Chile, Serie Geológica Básica. No. 115, Mapa Escala 1:100.000.

Németh, K., 2010. Monogenetic volcanic fields: Origin, sedimentary record, and relationship with polygenetic volcanism. In: Cañón-Tapia, E., Szakács, A., (Eds.), What is a volcano?: Geological Society of America Special Paper 470, pp. 43-66.

Park, J. B., Park, K. H., Cho, D. L. & Koh, G. W., 1999. Petrochemical classification of the Quaternary volcanic rocks in Cheju Island, Korea. Journal of the Geological Society of Korea 35, 253-264.

Pinel, V., Jaupart, C., 2000. The effect of edifice load on magma ascent beneath a volcano. In: Francis, P., Neuberg, J., Sparks, R.S. (Eds.), The Causes and Consequences of Eruptions of Andesite Volcanoes; Papers of a Discussion Meeting. Philosophical Transactions — Royal Society. Mathematical, Physical and Engineering Sciences 358, pp. 1515–1532.

Pinel, V., Jaupart, C., 2004. Magma storage and horizontal dyke injection beneath a volcanic edifice. Earth and Planetary Science Letters 221, 245-262. http://dx.doi.org/10.1016/S0012-821X(04)00076-7

Singer, B., Jicha, B.R., Harper, M.A., Naranjo, J.A., Lara, L.E., Moreno-Roa, H., 2008. Eruptive history, geochronology, and magmatic evolution of the Puyehue-Cordón Caulle volcanic complex, Chile. Geological Society of America Bulletin 120 (5-6), 599-618. http://dx.doi.org/10.1130/B26276.1

Stern, C.R., Moreno, H., López-Escobar, L., Clavero, J.E., Lara, L.E., Naranjo, J.A., Parada, M.A., Skewes, M.A., 2007. Chilean volcanoes. In: Moreno, T., Gibbons, W. (Eds.), The Geology of Chile. The Geological Society, London, pp. 147–178.

Sun, S., McDonough, W.F., 1989. Chemical and isotopic systematics of oceanic basalts; implications for mantle composition and processes. In: Saunders, A.D, Norry, J.M. (Eds.), Magmatism in the Ocean Basins, Special Publications .Geological Society of London 42, pp. 313– 345.

Takada, A., 1994a. Accumulation of magma in space and time by crack interaction, in Magmatic Systems, edited by M. P. Ryan, Academic Press, San Diego, California.

Takada, A., 1994b. The influence of regional stress and magmatic input on styles of monogenetic and polygenetic volcanism. Journal of Geophysical Research 99, 13,563-13,573. http://dx.doi.org/10.1029/94JB00494

Valentine, G.A., Gregg, T.K.P., 2008. Continental basaltic volcanoes – Processes and problems. Journal of Volcanology and Geothermal Research 177, 857-873. http://dx.doi.org/10.1016/j.jvolgeores.2008.01.050

Valentine, G.A., Perry, F.V., 2006. Decreasing magmatic footprints of individual volcanoes in a waning basaltic field. Geophysical Research Letters 33. http://dx.doi.org/10.1029/2006GL026743
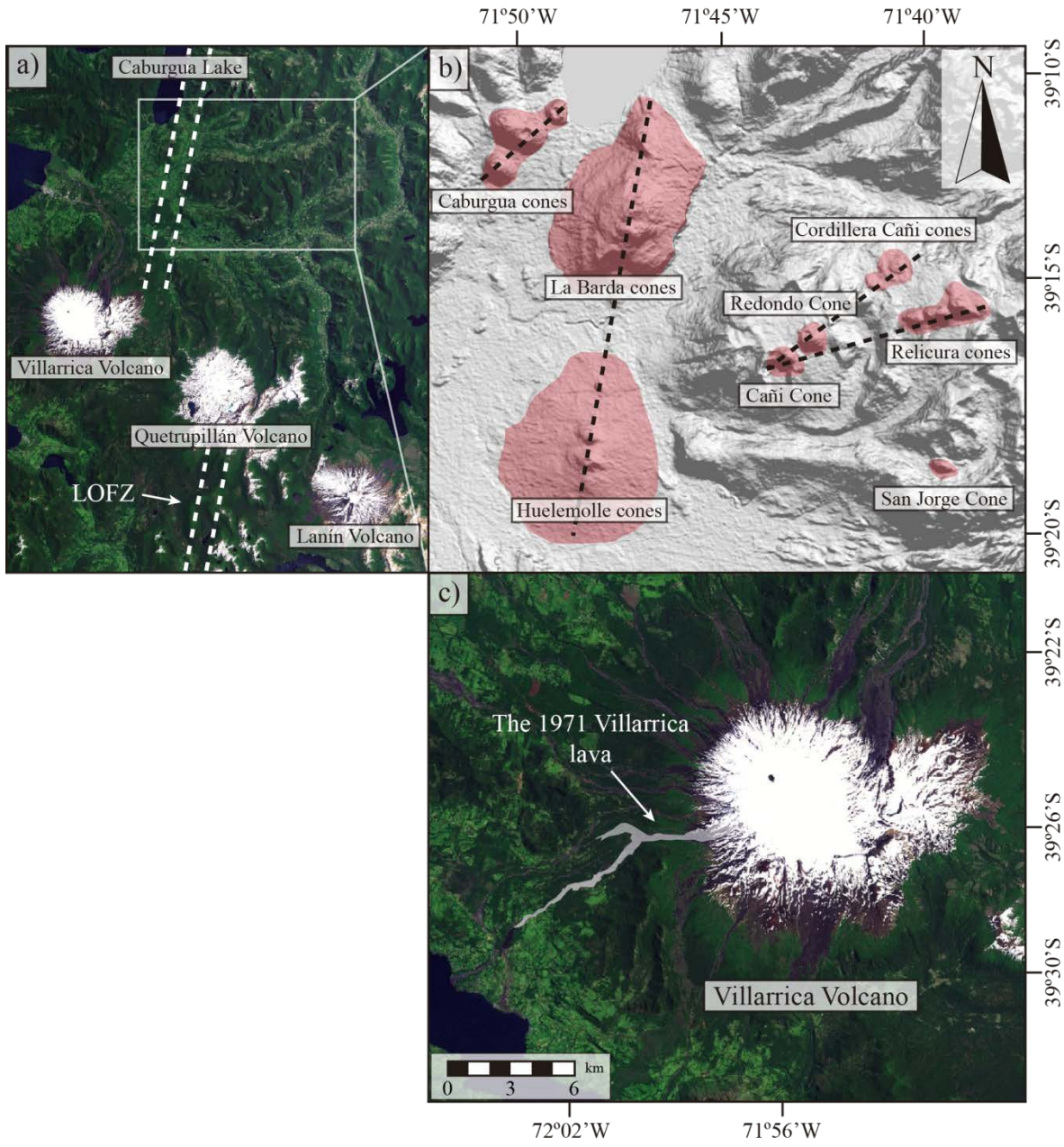
Figure 2.1. a) Location of the aligned Villarrica, Quetrupillán and Lanín Stratovolcanoes and the Liquiñe Ofqui Fault Zone (LOFZ; Cembrano et al., 1996) b) Distribution of the CHSEC cones. Dashed lines represent cone alignments that coincide with the NNE-striking faults and NE-striking tension cracks (Cembrano and Lara, 2009) associated to LOFZ c) Villarrica Volcano and the lava erupted during the 1971 eruption.

a)

b)
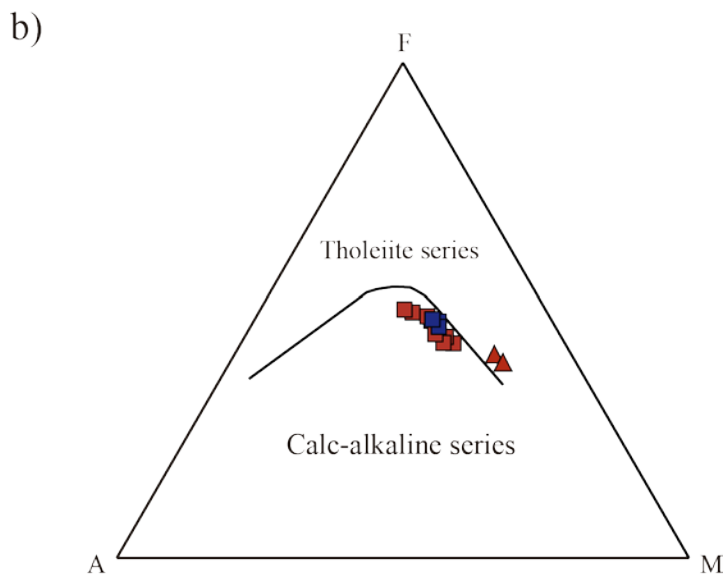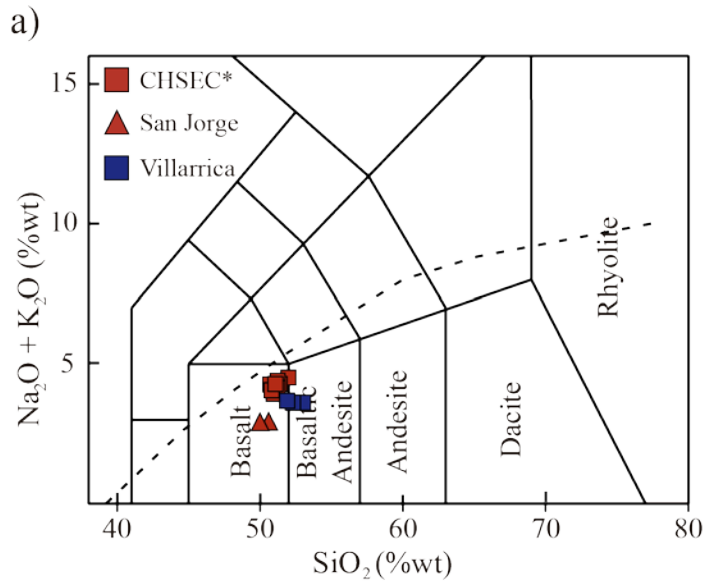
Figure 2.2. a) Total alkali vs. silica (Le Bas et al., 1986) plots of CHSEC basalts and the 1971 Villarrica basaltic andesite lavas. Boundary dashed-line between alkaline and subalkaline rocks is taken from Irvine & Baragar (1971); b) AFM diagram (Irvine & Baragar, 1971) showing calc-alkaline trend for most of the CHSEC and the 1971 Villarrica lava samples. Lavas of San Jorge cone exhibit tholeiitic affinities.
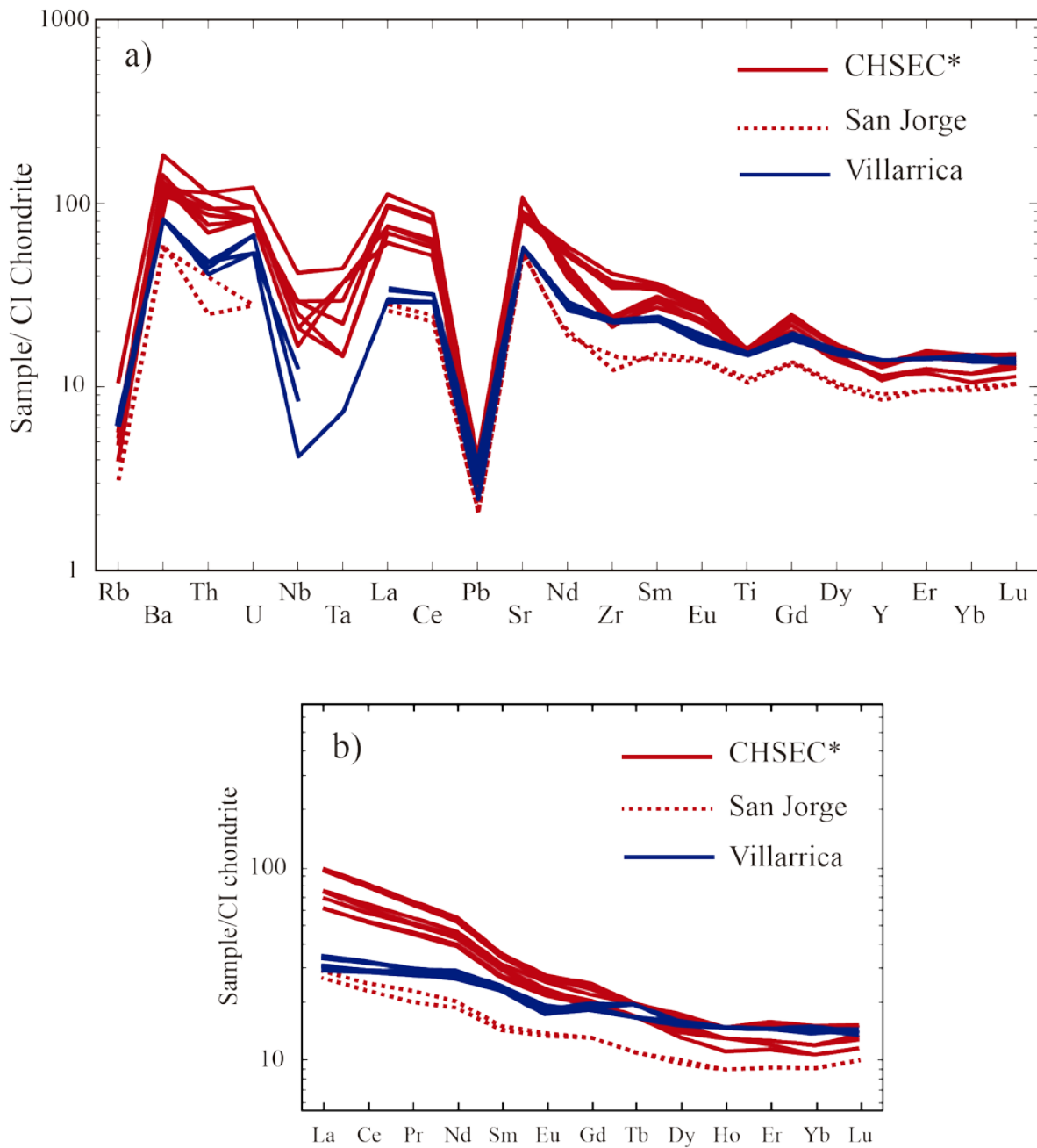
Figure 2.3. Chondrite-normalized (Sun and McDonough, 1989) spider diagram (a) and REE patterns (b) of samples from the small eruptive centers and the 1971 Villarrica lava. CHSEC* includes all samples taken from the small eruptive centers, except those form San Jorge cone.
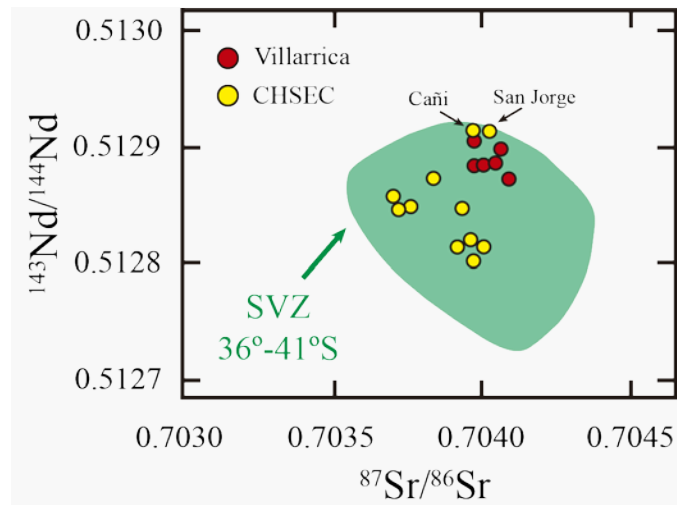
Figure 2.4. $^{143}Nd/^{144}Nd$ versus $^{87}Sr/^{86}Sr$ plots, for CHSEC and Villarrica Volcano samples. Field of SVZ between 37 and 41ºS are shown for comparison (data from López-Escobar et al., 1995 and references therein). Data of Villarrica and CHSEC samples obtained by Hickey-Vargas et al., (1989) are included.
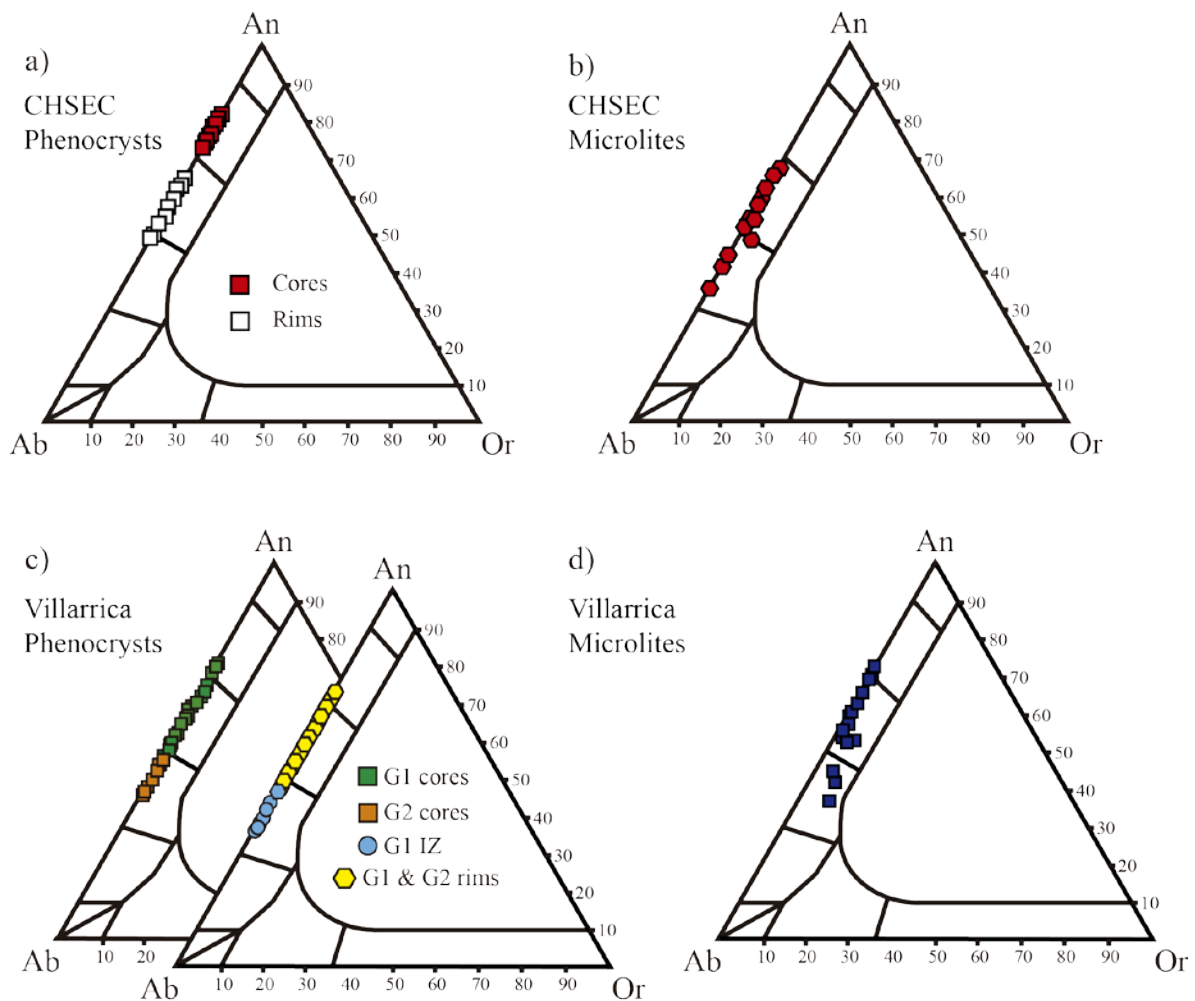
Figure 2.5. Plagioclase compositions of the studied CHSEC and 1971 Villarrica lava samples. G.1, G.2: Group 1 and Group 2 plagioclase phenocrysts; IZ: intermediate zone of phenocrysts.
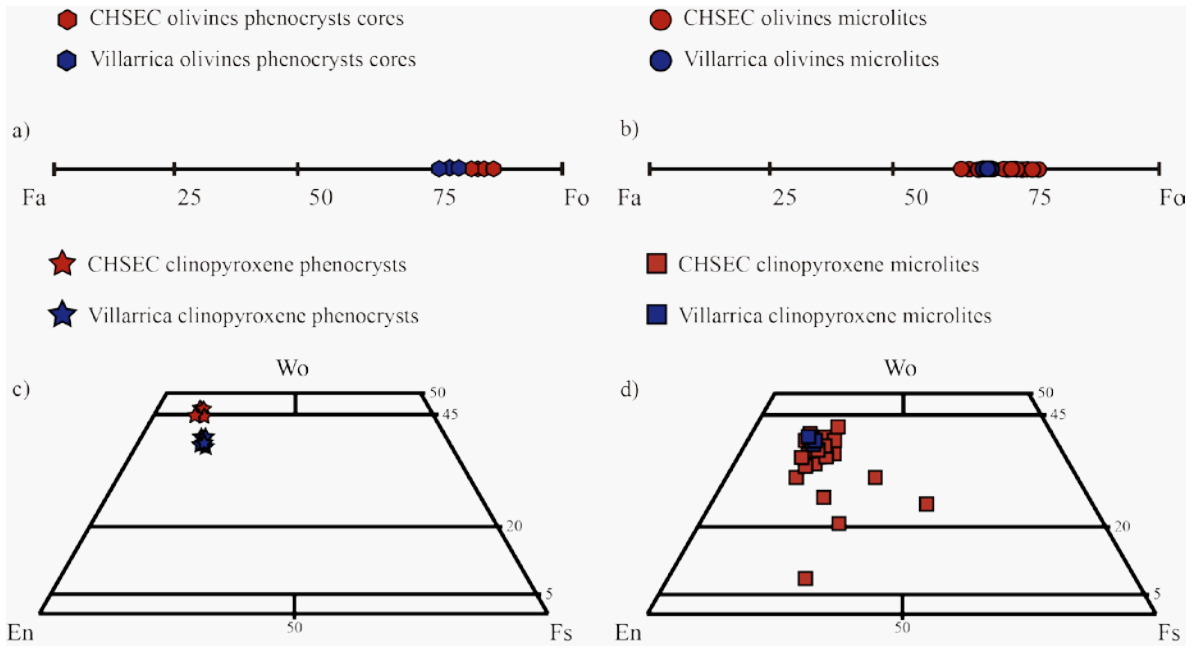
Figure 2.6. Olivine and clinopyroxene compositions of the studied samples. Compositions of olivine phenocrysts (a) and microlites (b) of CHSEC and 1971 Villarrica lava. Compositions of clinopyroxene phenocrysts (c) and microlites (d) of the CHSEC and 1971 Villarrica lava.
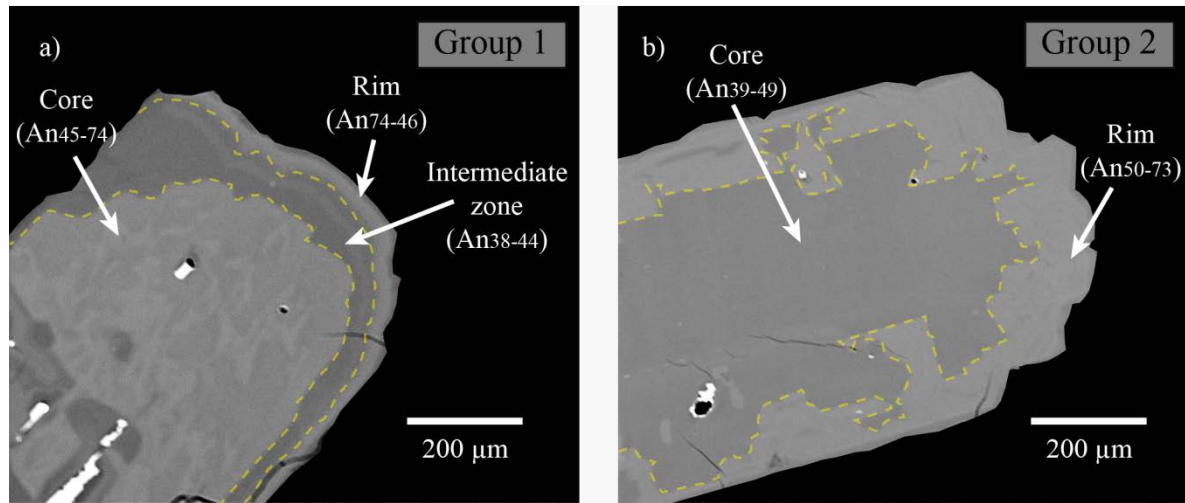
Figure 2.7. a) Core, intermediate, and rim zones from Group 1 plagioclase phenocryst. Disequilibrium features are recognized in core zone. b) Core and rim zones from Group 2 plagioclase phenocryst. Disequilibrium features are recognized in core zone.
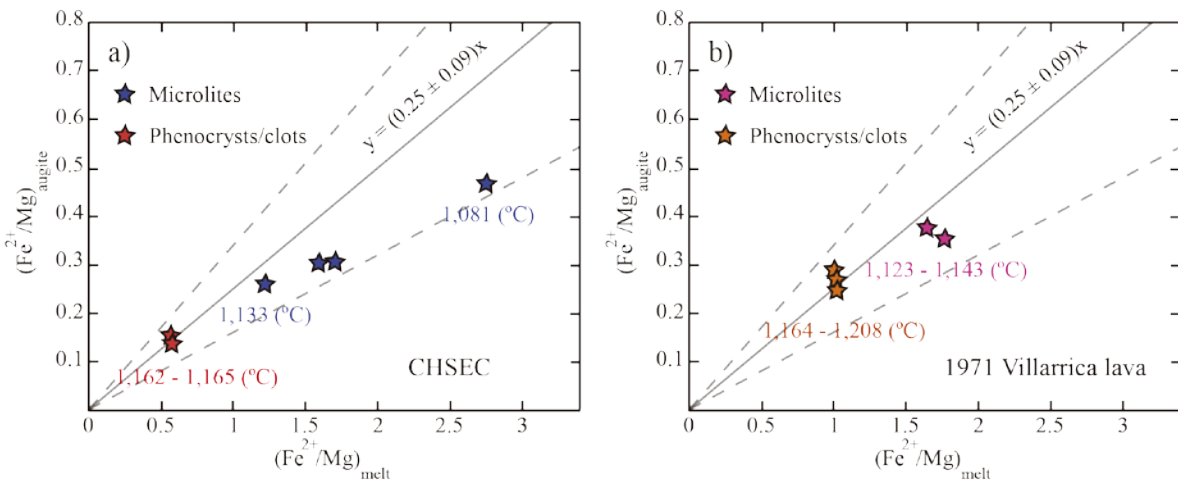
Figure 2.8. Augite-melt equilibrium compositions for CHSEC (a) and the 1971 Villarrica lava (b) inferred from plot of $(Fe^{2+}/Mg)_{augite}$ versus $(Fe^{2+}/Mg)_{melt}$ and the $^{cpx-liq}K_D(Fe^{2+}/Mg)$ for clinopyroxene in equilibrium with H_2O-saturated basic melt (continuous lines) and associated errors (dashed lines), following Grove's et al., (1997) equation. Temperatures obtained for olivine-augite equilibrium (Loucks, 1996) are shown.
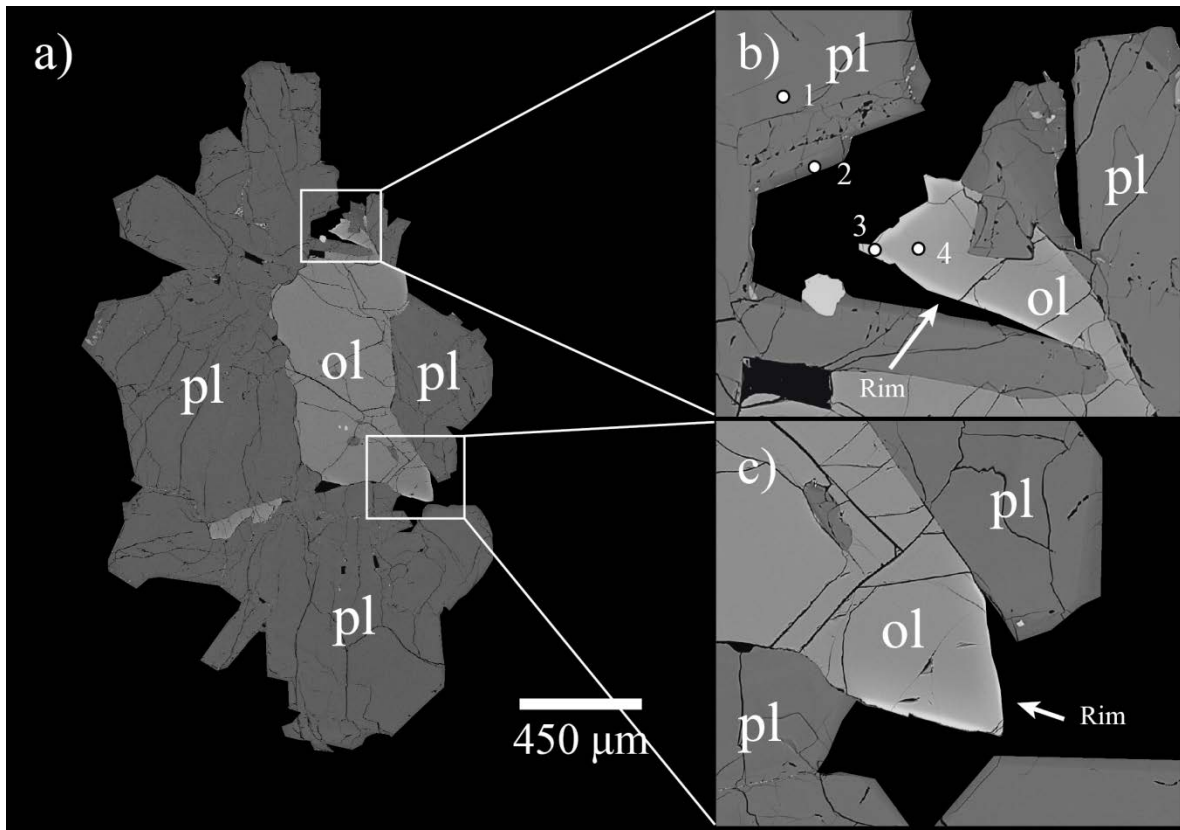
Figure 2.9. a) Crystal clot of plagioclase and olivine phenocrysts from CHSEC (sample HUEL-1). b) and c) show details of olivine and plagioclase crystal exhibiting thin rims only in the non-armored crystal faces (i.e. in contact with the matrix). Numbered spots indicate the sites of EPM analyses. Analyses 1 (HU-plph3), 2 (HU-plph5), 3 (HU-olph10), and 4 (HU-olph9) are shown in Table 2.5.
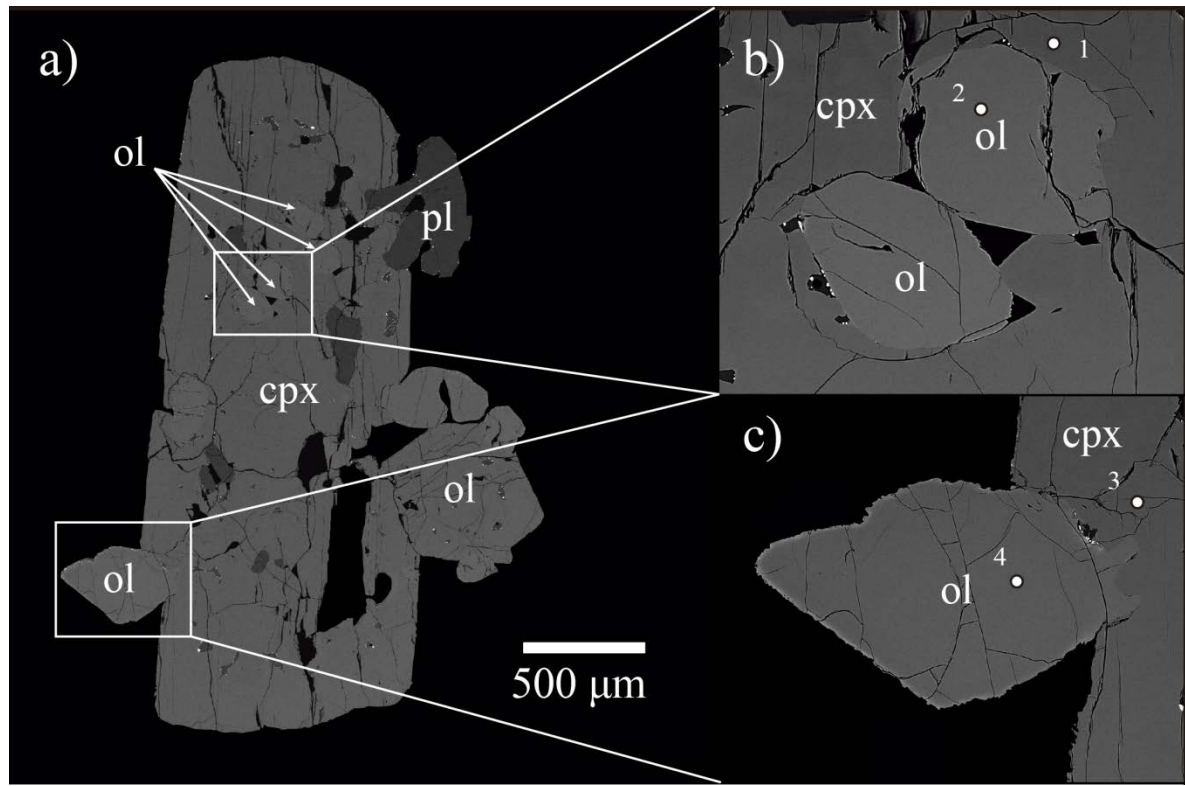
Figure 2.10. a) Crystal clot of plagioclase, olivine and clinopyroxene. b) Details of olivine chadacrysts that gave equilibrium temperatures with the neighboring clinopyroxene of 1,168 and 1,171 ± 6°C. c) Details showing thin rim in non-armored faces of the olivine. The equilibrium temperature of the olivine core-clinopyroxene is 1,209 ± 6°C. Numbered spots indicate the sites of EPM analyses. Analyses 1 (VI-pxph4), 2 (VI-olph4), 3 (VI-pxph5), and 4 (VI-olph5) are shown in Table 5.
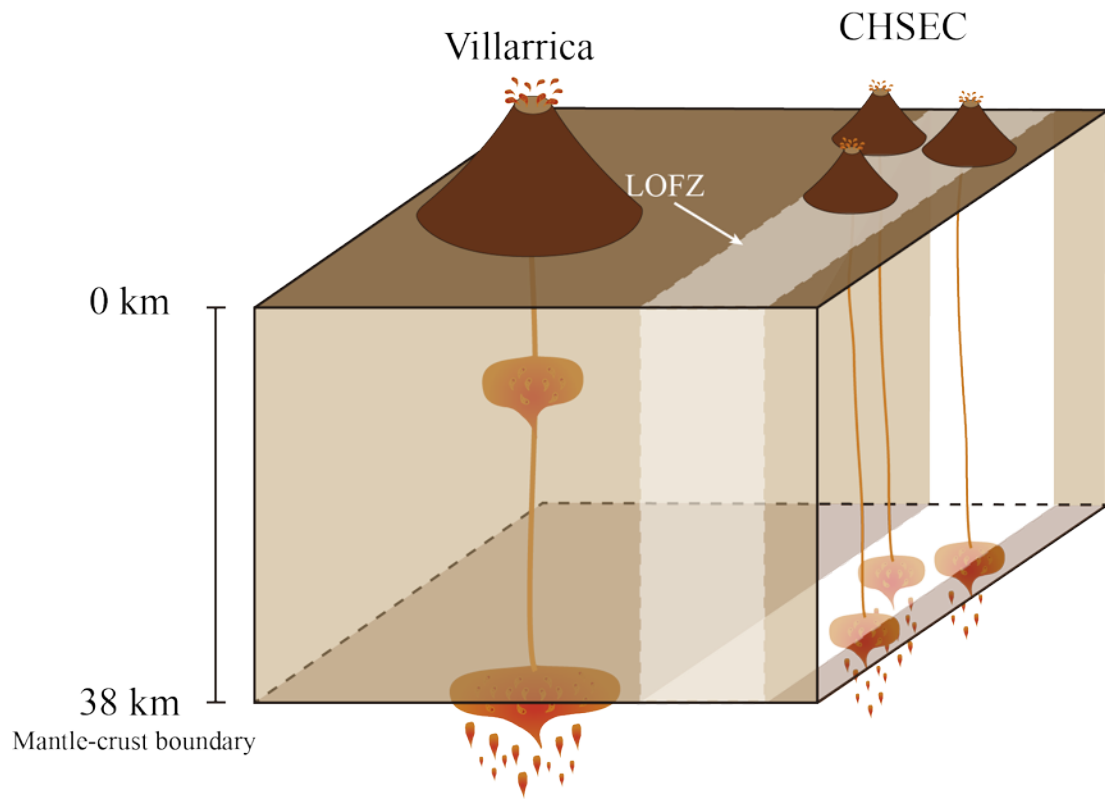
Figure 2.11. Schematic representation of the main characteristics of the CHSEC and Villarrica reservoirs. Both studied volcanic complexes would have deep reservoirs at the mantle-crust boundary, but unlike the Villarrica volcano, CHSEC do not have a shallow reservoir probably by role of the LOFZ as an efficient conduit for the ascending magma.
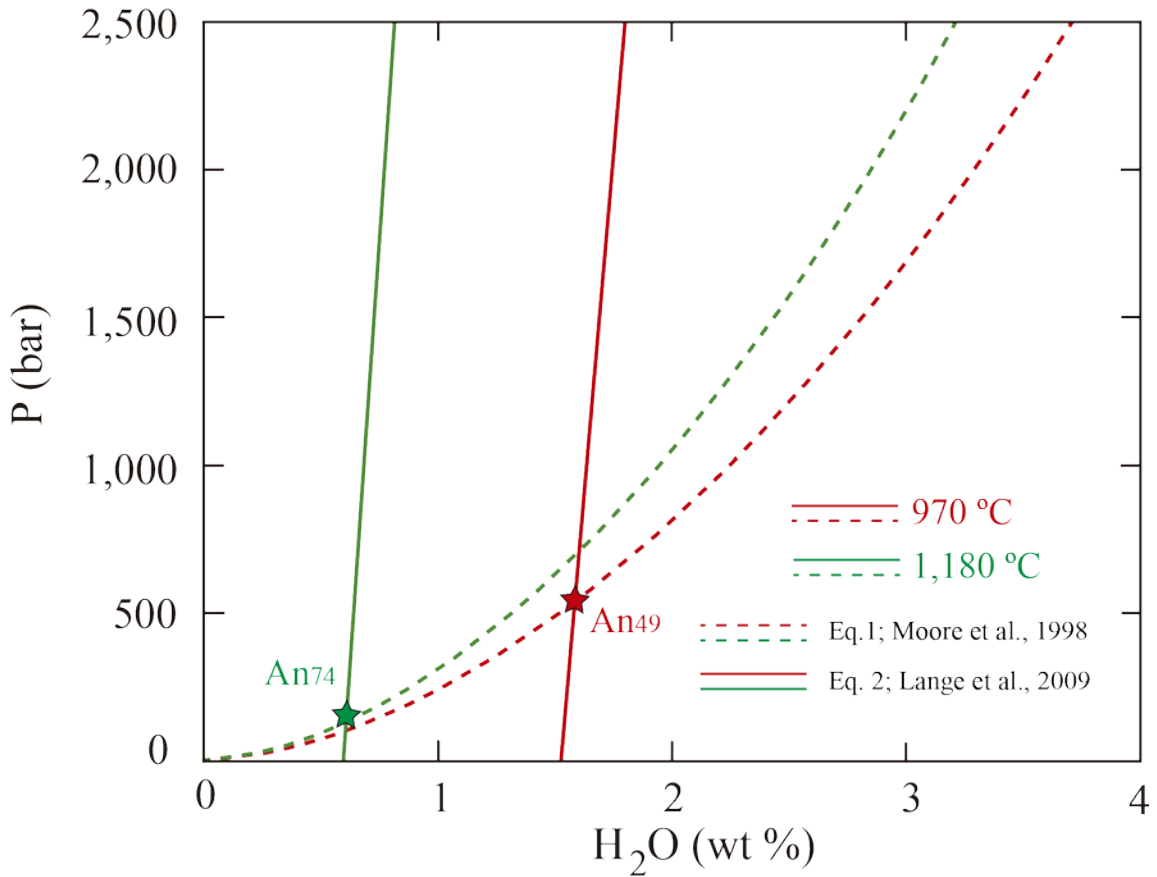
Figure A1. Numerical solution to determine variations of pressure conditions and H_2O concentration of the shallow reservoir associated with heating. A maximum pressure of 0.54 kbar for the shallow reservoir and a decompression of 0.4 kbar after 210°C heating were calculated. An exsolution of ~ 1 wt % H_2O was calculated for the mentioned heating. Continuous lines represent Lange´s et al. (2009) equation and dashed lines represent Moore´s et al. (1998) equation.

Table 2.1. Main features of CHSEC (cones of each SEC were ordened from north to south).

Eruptive center/cone	Max. height (m.a.s.l.)	Cone height (m)	Cone volume* (m^3)	Alignment (of the SEC)
Caburgua SEC				N50E
Caburgua 1	680	152	0.033	
Caburgua 2	751	244	0.104	
Caburgua 3	980	414	0.308	
Caburgua 4	755	331	0.135	
Huelemolle SEC				N15E
Huelemolle 1	560	102	0.013	
Huelemolle 2	820	450	1.91	
Huelemolle 3	859	489	2.076	
La Barda SEC				N10E
La Barda 1	678	271	0.054	
La Barda 2	941	444	0.203	
La Barda 3	1,209	696	4.69	
Relicura SEC				N70E
Relicura 1	1,537	98	0.002	
Relicura 2	1,648	287	0.011	
Relicura 3	1,571	263	0.005	
Relicura 4	1,598	290	0.005	
Relicura 5	1,507	176	0.003	
Cordillera Cañi				N45E
Cordillera Cañi 1	1,302	69	0.0004	
Cordillera Cañi 1	1,324	91	0.0009	
Other SECs				
Cañi cone	1,462	152	0.004	
Redondo cone	1,483	153	0.006	
San Jorge cone	1,120	150	0.004	

* The procedures for volume estimation were identical to those described by Aravena and Lahsen (2012).

Table 2.2 Whole rock analyses of samples from CHSEC and the 1971 Villarrica eruption. Only Caburgua, Huelemolle and San Jorge data were used in diagrams (Fig. 2.2 and 2.3).

	Caburgua					Huelemolle			
	Cab1-1	Cab1-2	Cab2-1	Cab2-2	Cab3-1	Huel-1	Huel-3	Huel-4	Huel-6
SiO2	50.26	49.88	50.24	51.31	50.78	49.96	50.95	51.77	50.12
Al2O3	17.48	17.5	17.5	17.45	17.56	17.73	18.22	17.76	18.19
TiO2	1.116	1.108	1.144	1.13	1.14	1.106	1.129	1.194	1.139
FeO	6.6	5.7	7.2	5.8	7.4	7.7	6.6	7.3	6
Fe2O3	2.97	3.72	2.45	4.33	2.38	2.18	3.53	2.88	3.74
MnO	0.149	0.149	0.15	0.156	0.154	0.156	0.161	0.159	0.153
MgO	6.8	6.71	6.33	7.45	7.06	5.66	5.67	4.6	4.74
CaO	8.68	8.92	8.79	8.84	8.72	9.4	9.55	8.91	9
Na2O	3.3	3.22	3.34	3.33	3.37	3.17	3.23	3.56	3.33
K2O	0.75	0.68	0.82	0.75	0.8	0.82	0.83	0.93	0.83
P2O5	0.29	0.31	0.34	0.33	0.34	0.41	0.4	0.43	0.43
LOI	-0.09	0.09	-0.34	0.03	-0.22	-0.16	-0.09	-0.23	0.44
Rb	10	9	12	9	11	13	13	14	13
Zr	79	81	92	85	89	132	137	143	136
Y	17	18	17	18	18	21	21	21	20
Nb	5	5	6	4	5	7	7	7	7
Ta	0.2	0.2	0.2	0.5	0.5	0.4	0.3	0.4	0.3
Ba	266	263	285	270	280	305	315	343	314
U	0.7	0.7	0.7	0.6	0.7	0.6	0.6	0.6	0.6
Th	2.7	2.7	3.3	2.5	2.7	2	2.8	2.2	2.2
Pb	7	7	8	10	8	9	10	10	10
La	14.4	16.3	17.7	14.4	17.6	22.7	23.1	23.1	22.6
Ce	31.5	35.1	39	31.7	37.1	48.1	49.3	49.7	47.9
Pr	4.14	4.65	5.03	4.24	4.71	5.87	6.13	6.03	5.92
Nd	17.6	19.3	21	18	20	24	24.9	24.5	23.6
Sm	3.9	4.3	4.6	4	4.4	5.1	5.2	5.2	5
Eu	1.2	1.25	1.41	1.26	1.3	1.49	1.49	1.53	1.45
Gd	3.8	3.9	4.3	4	3.9	4.7	4.6	4.9	4.7
Tb	0.6	0.6	0.7	0.6	0.6	0.7	0.7	0.7	0.7
Dy	3.2	3.5	3.7	3.4	3.4	4.2	4	4.1	4
Ho	0.6	0.7	0.7	0.7	0.7	0.8	0.8	0.8	0.8
Er	1.8	2	2	1.9	2	2.5	2.3	2.5	2.4
Tm	0.26	0.28	0.29	0.26	0.29	0.36	0.34	0.36	0.35
Yb	1.7	1.9	1.9	1.7	1.9	2.3	2.2	2.4	2.2
Lu	0.28	0.32	0.31	0.28	0.33	0.36	0.37	0.37	0.35

	San Jorge		Other SECs				
	Sani-1	Sani-3	Barda1-2	Rel1-2	Cañi-5	Rel-5	Cord2-2
SiO2	50.29	49.37	50.45	51.22	50.49	50.87	49.85
Al2O3	15.63	15.51	16.82	17.55	17.32	17.24	17.28
TiO2	0.804	0.763	1.077	1.167	1.023	0.994	1.165
FeO	6.3	7.7	6.9	8.4	7.3	7.9	4.8
Fe2O3	3.57	2.23	3.09	2.61	2.61	2.01	4.72
MnO	0.157	0.155	0.154	0.163	0.148	0.153	0.152
MgO	9.83	10.8	7.59	5.79	6.65	7.35	6.42
CaO	9.88	9.57	9.07	8.46	8.45	9.07	8.19
Na2O	2.5	2.46	3.13	3.29	3.17	3.08	3.28
K2O	0.41	0.41	0.74	1.11	0.85	0.79	1.23
P2O5	0.13	0.1	0.33	0.41	0.32	0.29	0.44
LOI	-0.12	-0.44	-0.08	-0.33	-0.18	-0.23	0.5
Rb	7	7	10	21	14	13	24
Zr	54	46	91	154	118	106	157
Y	14	13	18	21	18	18	21
Nb	< 1	< 1	3	6	4	4	10
Ta	< 0.1	0.8	0.1	0.4	0.2	0.3	0.6
Ba	140	132	260	397	305	280	440
U	0.2	0.2	0.6	0.8	0.5	0.5	0.9
Th	0.7	1.1	2.2	3.3	1.8	2	3.3
Pb	< 5	5	7	9	8	7	9
La	6	6.5	15	24.4	17.7	17.1	26.4
Ce	13.5	14.6	33	50.8	37	35.8	54.1
Pr	1.8	2.04	4.33	6.13	4.59	4.46	6.58
Nd	8.3	8.9	18.2	25.3	18.4	18.1	26.6
Sm	2.1	2.2	4	5.3	4.1	4.1	5.4
Eu	0.75	0.77	1.18	1.48	1.21	1.17	1.62
Gd	2.6	2.6	3.5	4.8	3.8	3.7	4.9
Tb	0.4	0.4	0.6	0.7	0.6	0.6	0.7
Dy	2.5	2.4	3.2	4.2	3.3	3.3	4.1
Ho	0.5	0.5	0.6	0.8	0.6	0.7	0.8
Er	1.5	1.5	1.9	2.4	1.8	1.9	2.3
Tm	0.23	0.23	0.27	0.34	0.27	0.28	0.35
Yb	1.5	1.5	1.7	2.1	1.7	1.8	2.2
Lu	0.25	0.25	0.28	0.34	0.27	0.29	0.34

	1971 Villarrica lava				
	1971 N6	1971 10 M1	1971 09	1971 30	R1971 DV
SiO2	52.85	51.92	52.47	52.93	51.76
Al2O3	16.76	16.68	16.71	16.77	16.59
TiO2	1.105	1.117	1.113	1.132	1.13
FeO	7.2	6.6	6.7	7.1	5.5
Fe2O3	3.05	3.17	3.31	2.83	4.55
MnO	0.157	0.154	0.154	0.154	0.154
MgO	6.39	5.95	6.1	6.02	6.1
CaO	9.76	9.57	9.61	9.63	9.55
Na2O	3.06	3.01	3.06	3.08	2.98
K2O	0.64	0.64	0.65	0.65	0.63
P2O5	0.21	0.23	0.23	0.18	0.2
LOI	-0.61	-0.47	-0.51	-0.55	-0.41
Rb	14	14	15	15	14
Zr	85	86	87	87	85
Y	22	22	22	22	21
Nb	1	1	1	2	1
Ta	< 0.1	< 0.1	0.1	< 0.1	< 0.1
Ba	201	199	200	198	197
U	0.4	0.4	0.4	0.5	0.4
Th	1.2	1.2	1.2	1.3	1.2
Pb	6	7	7	8	6
La	6.9	7.2	7.3	8	7
Ce	17.5	17.8	17.8	19.7	17.3
Pr	2.56	2.67	2.64	2.72	2.62
Nd	12	12.3	12.5	13.3	12.5
Sm	3.4	3.5	3.6	3.6	3.2
Eu	0.97	0.99	1.02	1.03	0.93
Gd	3.6	3.7	3.9	3.7	3.5
Tb	0.6	0.6	0.7	0.7	0.6
Dy	3.7	3.8	3.8	3.9	3.6
Ho	0.8	0.8	0.8	0.8	0.8
Er	2.3	2.3	2.3	2.3	2.4
Tm	0.37	0.36	0.35	0.35	0.37
Yb	2.4	2.3	2.3	2.2	2.3
Lu	0.34	0.33	0.35	0.35	0.32

Table 2.3. Isotopic data from SECs and the 1971 Villarrica eruption.

Eruptive center	Sample	87Sr/86Sr	143Nd/144Nd
Caburgua	Cab1-2	0.703762 ± 4	0.512849 ± 2
Huelemolle	Huel-1	0.703935 ± 4	0.512848 ± 2
La Barda	Barda1-2	0.703837 ± 4	0.512873 ± 2
Relicura	Rel1-2	0.704005 ± 4	0.512814 ± 2
Cañi	Cañi-5	0.703978 ± 4	0.512913 ± 2
Redondo	Red-5	0.703963 ± 4	0.512821 ± 2
C. Cañi	Cord2-2	0.703973 ± 4	0.512801 ± 2
San Jorge	SanJ-3	0.704028 ± 5	0.512913 ± 4

Table 2.4. Pressure and temperatures obtained from clots of crystals, oikocryst-chadacryst and microlites.

Eruptive center	T (± 6 ℃; Loucks, 1996)	P (kbar; Köhler and Brey, 1990)	Depth (km)
Villarrica			
Clot of crystals	1,208	4.6 - 9.8	18.9 - 34.5
Oikocryst-chadacryst	1,168-1,175	0 - 2.4	0 - 12.2
Microlites	1,123-1,148	-	
CHSEC			
Phenocrysts (in contact)	1,162-1,165	7.7 – 14.4	28.3 - 48.5
Microlites	1,081-1,133	-	

Table 5. Representative chemical analyses of minerals from CHSEC and the 1971 Villarrica eruption.

	Plagioclases				Olivines			
	HU-plph3	HU-plph5	SJ-plph3		VI-olph5	VI-olph4	HU-olph10	HU-olph9
SiO2	47.27	46.988	47.728	SiO2	38.864	38.664	38.794	39.526
Na2O	1.935	1.394	1.561	Al2O3	0.045	0.003	0.006	0.003
Al2O3	34.099	34.656	33.46	MgO	39.779	39.709	40.767	43.571
K2O	0.053	0.024	0.026	CaO	0.236	0.259	0.208	0.159
CaO	17.306	17.89	17.415	MnO	0.445	0.399	0.026	0.026
Total	100.663	100.952	100.190	FeO	21.175	21.892	20.835	17.897
XAn	90.51	77.258	92.418	Total	100.544	100.926	100.636	101.182
XAb	9.15	22.681	7.498	XFo	77	76	78	81
XOr	0.33	0.06	0.082	XFa	23	23	22	19

	Pyroxenes				Chromian-spinels		
	VI-pxph5	VI-pxph4	SJ-pxph3		CA-opin1	HU-opin1	VI-opin1
SiO2	51.774	52.154	52.526	Al2O3	27.616	26.98	12.319
Al2O3	2.791	2.666	2.917	MgO	12.833	12.11	7.882
MgO	16.804	16.877	16.962	CaO	0.007	0	0
CaO	18.42	19.562	22.641	TiO2	0.875	0.21	0.534
TiO2	0.574	0.574	0.3	Cr2O3	27.605	25.4	33.47
Cr2O3	0.452	0.452	0.381	FeO	12.02	35.28	12.83
MnO	0.275	0.204	0.15	Fe2O3	18.64	0	32.37
FeO	8.626	7.477	4.11	NiO	0.27	0.2	0.087
Fe2O3	0.076	0.15	0.961	Total	99.866	100.18	99.49
Total	99.792	100.142	100.948	#Mg	57.44	37.96	27.34
XEn	48.04	47.80	47.723	#Cr	33.4	38.71	61.66
XFs	11.94	12.13	6.494				
XWo	40.02	39.94	45.784				

For these and other clinopyroxenes and chromian-spinel inclusions the values of Cr-spinels Fe^{2+} and Fe^{3+} were obtained following Droop's (1987) proposition.

CAPÍTULO 3

TRANSIENT SHALLOW RESERVOIRS BENEATH MONOGENETIC VOLCANOES: CONSTRAINTS FROM MAGMA RESIDENCE OF CABURGUA CONES IN THE ANDEAN SOUTHERN VOLCANIC ZONE

Morgado, E.[1]*, Parada, M. A.[1], Morgan, D.J.[2], Gutiérrez, F.[1, 3], Castruccio, A.[1], Contreras, C.[1],

[1] Departamento de Geología, Facultad de Ciencias Físicas y Matemáticas, Universidad de Chile, Chile/ Centro de Excelencia en Geotermia de los Andes (CEGA)

[2] Institute of Geophysics and Tectonics, School of Earth and Environment, University of Leeds, Leeds LS2 9JT, UK

[3] Advanced Mining Technology Center, Universidad de Chile

* Corresponding author at: Centro de Excelencia de Geotermia de los Andes (CEGA), Departamento de Geología, Facultad de Ciencias Físicas y Matemáticas, Universidad de Chile, Santiago 8370450, Chile.

E-mail addresses: emorgado@ing.uchile.cl (E. Morgado), maparada@cec.uchile.cl (M. Parada), d.j.morgan@leeds.ac.uk (D. Morgan), clcontre@ug.uchile.cl, (C. Contreras), frgutier@ing.uchile.cl (F. Gutiérrez), acastruc@ing.uchile.cl (A. Castruccio).

Abstract

It is well known that small eruptive centers mostly have more primitive lavas than those associated to stratovolcanoes. Shorter magma residence in the crust has been proposed to explain this, which is consistent with a direct magma transport from depth without shallow reservoirs. Here, we use diffusion modeling of zonation patterns in olivine phenocrysts, thermobarometry and MELTS simulations to estimate the time of magma residence of lavas of Caburgua cones (39º10'S) and

conditions of magma reservoir in the crust. The minimum timescales vary from 11.3 to 78 days and only can be explained by the existence of at least one shallow reservoir otherwise, the ascending magma from the deep crust would be frozen before reaching the surface. The maximum time intervals of olivine rim formation are up to 4 months, representing the highest magma residence. However, these intervals are shorter than those from the nearby more differentiated Villarrica stratovolcano, which has a dominant basaltic andesite composition. For Caburgua cones the existence of a transient reservoir is deduced from numerical modeling, and differs from the long-lived reservoir beneath the Villarrica stratovolcano. The presence of Liquiñe-Ofqui Fault Zone beneath the small eruptive centers in Andean Southern Volcanic Zone would facilitate the magma ascent and then decrease the magma residence in the crust.

3.1 Introduction

For developing monogentic cones, small volumes of primary magma ($0.01\ km^3/yr$ or less) are necessary; however these small-volume ascending magmas can be frozen in just few days (Németh, 2010). Two hypotheses were proposed (Németh, 2010) for understanding small-size continental volcanism: 1) short-lived volcanism, where vertical conduits transport primitive magmas from a deep source with variable crystallization degrees (e.g. Auckland Volcanic Field; Smith et al., 2008) and 2) long-lived volcanism, where a shallow melt accumulation zone below the volcano took place (e.g. Jorullo volcano; Johnson et al., 2008). In general terms, textural features found in samples from stratovolcano lavas are more

complexes (normal and reverse zoning, disequilibrium features, etc.) than those related to small eruptive centers (e.g., López-Escobar et al., 1995a; Morgado et al., 2015). In the Andean Southern Volcanic Zone (SVZ) of the Andes, dissimilarities in upper crustal residence times between the short magma residence of small eruptive centers and the larger magma residence of the neighboring stratovolcanoes have been suggested by Lara et al. (2006) for the Cordón Caulle-Puyehue volcanic complex. They also attribute to difference in magma residence as one of the causes for explaining the compositional differences between the primitive lavas of small centers and the most differentiated volcanic materials of the stratovolcanoes.

Magma ascent processes and residence times have been studied using different techniques: U-Th-Ra isotopic disequilibrium in magma (Condomines et al., 1998), seismicity during eruptive periods (Scandone and Malone, 1985; Lees and Crosson, 1989; Endo et al., 1996), presence of dense xenoliths carried to surface by magma (e.g. Spera, 1984; Sparks et al., 2006), reaction rim growth on amphibole phenocrysts (Rutherford and Hill, 1993), and hydrogen loss profiles in olivine (Demouchy et al., 2006). One of the most recent methods to constraint the timescales of the pre-eruptive processes is that based on modeling of element diffusion diffusion through crystals (e.g. Zellmer et al., 1999; Morgan et al., 2004; Costa and Dungan, 2005; Chamberlain et al., 2014). This technique consists in finite element-based modeling of elements diffusion through a crystal with an initial profile composition. The element diffusion ceases when an equilibrium crystal profile composition is reached or aborted. This method allows calculating short-lived (e.g., Costa and Dungan, 2005; Martin et al., 2008) and long-lived (e.g.

Morgan and Blake, 2006) events prior to eruption and in some occasions short-lived events can be correlated with volcanogenic seismic data (e.g., Kahl et al., 2011; 2013).

This study focuses on olivine residence time of lava from Caburgua monogenetic cones, a member of Caburgua-Huelemolle Small Eruptive Centers (CHSEC) in the Andean Southern Volcanic Zone. Month-scale olivine residence times are calculated for a transient upper-crustal reservoir, which contrasts with a permanent reservoir of the nearby Villarrica stratovolcano.

3.2 Analytical Procedure

Two samples from Caburgua (CAB1-1; CAB2-2) were collected from one *Pahoehoe* lava. Compositional profiles were measured in three olivine crystals using an electron microprobe at School of Geosciences, University of Edinburgh (Cameca SX100). The analytical conditions consisted in an accelerating potential of 15 kV and electron beam current of 4 nA for major elements and 100 nA for minor and trace elements. Counting times for major elements were 20 seconds on peak and 10 seconds on background. Also, higher resolutions of Fe-Mg diffusion profiles were obtained through back-scattered electron compositional contrast images, using a Scanning Electron Microscope (SEM) at University of Chile (FEI Quanta 250), calibrated with the electron microprobe analyses. Crystallographic orientations were determined using electron back-scatter diffraction at School of Earth and Environment, University of Leeds.

3.3 Geology, mineralogy and P,T conditions of the Caburgua cones

Caburgua cones, which form part of CHSEC (Fig. 3.1), are built over the Liquiñe-Ofqui Fault Zone (LOFZ), a major intra-arc structure that controls the distribution of numerous volcanic edifice of the SVZ (e.g., López-Escobar et al., 1995a; Lara et al., 2006; Cembrano and Lara, 2009). The Caburgua cones are composed of five edifices of basaltic cones and lavas (Hickey-Vargas et al., 1989; López-Escobar et al., 1995b; Moreno and Lara, 2008) of up to 0.3 km^3 (Morgado et al., 2015) with variable height between 152 and 414 m.a.s.l. and volumes between 0.033 and 0.308 km^3. They have variable contents of phenocrysts (7-14%) in a groundmass with <1% glass. The olivine phenocrysts (Fo$_{82-84}$) exhibit a thin rim of Fo$_{77.5-78.5}$ and microlites have compositions of Fo$_{53-75}$. Plagioclase occurs as phenocrysts of An$_{73-76}$ and microlites of An$_{48-63}$. Clinopyroxenes are scarce and occur as phenocrysts with compositions of Wo$_{44-46}$, En$_{45-47}$, Fs$_{7-9}$ and microlites with compositions of composition of Wo$_{8-40}$, En$_{37-63}$, Fs$_{13-31}$. Chromian-spinels occur as inclusions in olivine phenocrysts and have variable #Cr and #Mg of 27-34, and 33-59, respectively. Titanomagnetites occur as microlites of composition Mt$_{35-42}$, Usp$_{58-65}$.

Using Loucks's (1996) thermometer and Kohler and Brey´s (1990) barometer, olivine-augite antecrystic pairs of a Caburgua lava sample gave equilibrium temperatures with a common melt composition between 1,162 and 1,165 ±6 °C and pressure between 7.7 and 14.4 kbar. The values of the calculated pressure range are similar to the ~10 kbar (~38 km) for the mantle-crust boundary beneath the arc at these latitudes (Folguera et al., 2007), thus a reservoir at these depths is assumed

(Morgado et al. 2015). Mineral formed during the ascent from deep reservoir and/or in an intermediate reservoir are not identified, except the rims around olivine phenocrysts. In fact, the stability fields of olivines with the composition of the rims were calculated by MELTS (Ghiorso and Sack, 1995; Asimow and Ghiorso, 1998) at different water content and NNO oxygen fugacity conditions (Fig. 3.2). The rim formation is then constrained at a pressure below 2.5 kbar and temperatures between 1,130 and 1,180°C. Finally, olivine-augite microlites pairs formed during syn-eruptive crystallization gave temperatures between 1,081 and 1,133 ± 6°C. Slightly higher temperatures between 1,130 and 1,137 °C were obtained by MELTS for olivine and clinopyroxene microlite compositions.

3.4 Rate of ascent

3.4.1 Basis

Diffusion can be described and modeled using the Fick's (1855) second law

$$\frac{\partial C(x,t)}{\partial t} = \frac{\partial}{\partial x}\left(D \frac{\partial C(x,t)}{\partial x} \right) \quad \text{Eq. 1}$$

where C is composition, t is time, and D is the diffusion coefficient that may be described by an Arrhenian relation (e.g., Coogan et al., 2005; Dohmen and Chakraborty, 2007).and depends on crystallographic orientation, temperature, pressure, composition and oxygen fugacity.

Mg-Fe (inter)diffusion in olivine along plane [001] is calculated by Eq. 2 (Dohmen and Chakraborty 2007) and its expected value is about six times faster than [100] and [010] (Dohmen et al., 2003)

$$D_{\text{olivine}}^{\text{Fe}-\text{Mg}} = 10^{-9.21} \cdot \left(\frac{f_{O_2}}{10^{-7}}\right)^{\frac{1}{6}} \cdot 10^{3 \cdot (X_{\text{Fe}}-0.1)} \exp\left(-\frac{201{,}000 + (P - 10^5) \cdot 7 \cdot 10^{-6}}{RT}\right) \quad \text{Eq. 2}$$

where X_{Fe} is the mole fraction of fayalite component, P is pressure (Pa), f_{O_2} is oxygen fugacity, T is temperature (K) and R is the universal gas constant ($\frac{J}{mol \cdot K}$).

We can model the diffusion coefficient for any crystallographic orientation using Philibert's (1991) proposition.

$$D_{\text{trav}}^{\text{Fe}-\text{Mg}} = D_{[100]}^{\text{Fe}-\text{Mg}} (\cos(\alpha))^2 + D_{[010]}^{\text{Fe}-\text{Mg}} (\cos(\beta))^2 + D_{[001]}^{\text{Fe}-\text{Mg}} (\cos(\gamma))^2 \quad \text{Eq. 3}$$

where α, β and γ are angles between the traverse and the a-, b- and c- axes of the olivine, D_a^i is the diffusion coefficient parallel to "a" axis direction of the element "i".

Concentration profiles (Fe, Mg, Si, Ni, Mn, Al and Ca) were measured along different directions in olivine crystals, with a spacing varying between 5 and 10 micrometers using EMPA. For determining if the zoning has been produced by diffusion or by a rim overgrowth, we use the Costa's et al., (2008) expression

$$x^a/x^c \approx \sqrt{D_a/D_c} \quad \text{Eq. 4}$$

where x^a, x^b are the widths of zoning along different directions. Diffusion process is determined when the ratio of Eq.4 is close to the value calculated from diffusion data.

3.4.2 Results

The factors affecting the uncertainties associated to timescale determinations using zoning profiles have been determined (e.g., Costa et al., 2008; Costa and Morgan, 2010) being the most important the following: (i) difficulty of precisely measuring

diffusion coefficients; (ii) uncertainties associated to temperature (diffusion coefficients vary exponentially with temperature), (iii) initial and boundary conditions and (iv) other variables such as P, fO_2. One of the most important problems concerning the estimation of the magmatic zoned crystal residence is determine the thermodynamic conditions of the zonation and where the zonation pattern was initiated (Rutherford, 2008) or developed in the plumbing system. In order to obtain the thermodynamic conditions necessary for calculating the magmatic timescales associated to the olivine rim formation, the measured olivine rim composition were reproduced by MELTS at different P, T, oxygen fugacity and dissolved H2O wt % contents. The compositional profiles were obtained in two crystals of sample CAB2-2. The shortest time interval for olivine rim formation is 7.1 days was obtained in melt at the maximum calculated T of 1,180 ºC and P of 1.8 kbar, NNO f_{O_2} buffer and 0 wt % dissolved H_2O (Fig. 3.2). A maximum time interval of olivine rim formation between 88 and 121 days (Table 1, Fig. 3.3) are obtained using temperature of 1,130 ºC (syn-eruptive temperatures), 0.07 kbar (lower pressure implies slower diffusivity), 0.5 wt % of dissolved H_2O and NNO f_{O_2} buffer. If an intermediate reservoir does not exist, the calculated timescales represent the ascent times. Assuming variations in melt temperature during the olivine rim formation in a cooling ascending magma an average temperature should be considered (Lasaga and Jiang, 1995; Costa et al., 2008). Taking the average temperature of 1,160 °C resulting from the maximum MELTS temperature for the rim growth (1,180 °C) and the syn-eruptive olivine-clinopyroxene temperature (1,130 °C), the calculated time interval of olivine rim formation are between 11.3 and 78 days (Table 1, Fig 3.3).

3.5 Discusion

3.5.1 Transient shallow reservoir

If we assume that Caburgua cones belong to a short-lived volcanic system as a consequence of direct dykes transport of magmas from a deep source (base of the crust), the calculated timescales of olivine rim formation would only represent magma ascent time form a depth equivalent to 1.8 kbar and the maximum associated ascent rates (related to the minimum time) would be 0.6 km/day. Menand et al. (2015) calculated the minimum rate of magma transport in the crust to avoid freezing of ~0.01 km^3/yr, which is substantially larger than maximum transport velocity for the Caburgua magmas of 3.3·10^{-6} km³/yr calculated with a cylindrical conduit with a radius of 25 m. In other words, if the minimum time for rim formation only represented ascent time, the ascending magma would have been frozen before reaching the surface. Consequently, a substantially higher ascent rate than 0.6 km/day is necessary to avoid freezing. This implies the existence of a pause or transient reservoir in the magma ascent to surface whose P,T conditions given by the olivine rim formation are P <2.5 kbar and T <1,180°C (Fig. 3.2). The maximum time interval calculated for the olivine rim formation is 121 days, which would represent the maximum residence time in the shallow reservoir.

Renewal of the volcanic activity in a Caburgua monogenetic cone is unlikely because the minimum necessary magma input rate (R_{min}) to sustain the temperature of a very small reservoir above the solidus is about 0.005 km^3/yr (Gelman et al., 2013). If this magma input rate was valid for Caburgua, then the

period between eruptions should be about 3.3 years by considering the volume of magma recharge was about five times the extruded magma volume (0.13 km³; White et al., 2006) and the following expression:

$$t \ = \ \frac{V_{int}}{R_{min}} \quad Eq.\,5$$

where t is time (years), V_{int} is the intruded volume (km³). The calculated period could indicate the interval between the clustered cone constructions if all of them were formed from a common transient reservoir.

3.6 Conclusions

Caburgua cones are examples of small eruptive centers built over the intra-arc Liquiñe-Ofqui Fault Zone developed along the Andean Southern Volcanic Zone. They have at least two reservoirs of contrasting depths in the crust. The deepest reservoir, located at the mantle-crust boundary, and a shallow transient reservoir, at a depth equivalent to <2.5 kbar (Fig. 3.4). The magma residence time in the shallow reservoir can be estimated from the time of olivine phenocryst rim formation, which is shorter than 121 days before the eruption. The calculated magma residence in the upper crust is strongly influenced by a low magma input rate allowing a premature magma freezing and it is much lower than decadal timescale magma residence in the shallow reservoir calculated for the nearby Villarrica stratovolcano (Lohmar et al., 2012). The presence of short-lived transient reservoir could explain why magmas of small eruptive centers are evacuated by numerous neighboring vents in contrast with a single-vent evacuation of

stratovolcanoes, which have permanent and larger reservoir because of high magma input rates. We hypothesize that Caburgua lavas as well as other small eruptive center lavas of the Southern Volcanic Zone can reach the surface after short residence times because of the influence of the Liquiñe-Ofqui Fault Zone below the volcanic complex as a natural pathway.

Acknowledgments

References

Annen, C., 2009. From plutons to magma chambers: Thermal constraints on the accumulation of eruptible silicic magma in the upper crust. Earth and Planetary Science Letters v. 284, p. 409-416.

Asimow, P.D., Ghiorso, M.S., 1998. Algorithmic modifications extending melts to calculate subsolidus phase relations. American Mineralogist, v.83, p.1127–1131.

Cembrano, J., Lara, L., 2009. The link between volcanism and tectonics in the southern volcanic zone of the Chilean Andes: A review. Tectonophysics, v.471, p.96-113.

Chamberlain, K.J.; Morgan, D.J.; Wilson, C.J.N., 2014. Timescales of mixing and mobilisation in the Bishop Tuff magma body: Perspectives from diffusion chronometry. Contributions to Mineralogy and Petrology v. 168, p.1-24. doi: 10.1007/s00410-014-1034-2

Condomines, M., Hemond, C., Allegre, C.J., 1988. U-Th-Ra radioactive disequilibria and magmatic processes. Earth and Planetary Science Letters, v.90, p.243-262.

Coogan, L.A., Hain, A., Stahl, S., Chakraborty, S., 2005. Experimental determination of the diffusion coefficient for calcium in olivine between 900 °C and 1500 °C. Geochimica and Cosmochimica Acta, v.69, p.3683–3694.

Costa F., Dungan, M., 2005. Short time scales of magmatic assimilation from diffusion modelling of multiple elements in olivine. Geology, v.33, 837-840.

Costa, F., Dohmen, R., Chakraborty, S., 2008. Time scales of magmatic processes from modeling the zoning patterns of crystals. Reviews in Mineralogy and Geochemistry, v.69, p. 545–594.

Costa, F., Morgan, D. J., 2010. Timescales of Magmatic Processes, In: Dosseto A; Turner S; Van-Orman J (Ed) Timescales of Magmatic Processes, Wiley-Blackwell.

Demouchy, S., Jacobsen, S.D., Gaillard, F., Stem, C.R., 2006. Rapid magma ascent recorded by water diffusion profiles in mantle olivine. Geology, v.34, p.429-432.

Dohmen, R., Becker H.-W., Chakraborty, S., 2003. Point defect equilibration and diffusion in olivine at low temperatures (T<1000 ºC), European Journal of Mineralogy, v.15, p.42.

Dohmen, R., Chakraborty, S., 2007. Fe−Mg diffusion in olivine II: point defect chemistry, change of diffusion mechanisms and a model for calculation of diffusion coefficients in natural olivine. Physics and Chemistry of Minerals v. 34, p.409−430.

Erlund, E.J., Cashman, K.V., Wallace, P.J., Pioli, L., Rosi, M., Johnson, E., Delgado Granados, H., 2010. Compositional evolution of magma from Parícutin Volcano, Mexico: The tephra record. Journal of Volcanology and Geothermal Research v. 197, p. 167-187.

Endo, E.T., Murray, T.L., Power, J.A., 1996. A comparison of pre-eruption, real-time seismic amplitude measurements for eruptions at Mount St. Helens, Redoubt Volcano, Mount Spurr, and Mount Pinatubo. *In:* Fire & Mud: eruptions and lahars of Mount Pinatubo, Philippines. Newhall CG, Punongbayan RS (eds) University of Washington Press, Seattle, p. 233-246.

Fick, A., 1855. On liquid diffusion. Philosophical Magazine and Journal of Science, v.10, p. 30-39.

Folguera, A., Introcaso, A., Giménez, M., Ruiz, F., Martínez, P., Tunstall, C., García Morabito, E., Ramos, V., 2007. Crustal attenuation in the Southern Andean retroarc (38°−39º30′ S) determined from tectonic and gravimetric studies: The Lonco-Luán asthenospheric anomaly. Tectonophysics 439, p. 129-147.

Ghiorso, M.S., Sack, R.O., 1995. Chemical mass transfer in magmatic processes: IV. A revised and internally consistent thermodynamic model for the interpolation and extrapolation of liquid–solid equilibria in magmatic systems at elevated temperatures and pressures. Contributions to Mineralogy and Petrology v. 119, p. 197–212.

Hickey-Vargas, R., Moreno, H., López Escobar, L., Frey, F., 1989. Geochemical variations in Andean basaltic and silicic lavas from the Villarrica–Lanín volcanic chain (39.5°S): an evaluation of source heterogeneity, fractional crystallization and crustal assimilation. Contributions to Mineralogy and Petrology v.103, p.361–386.

Johnson, E.R., Wallace, P.J., Cashman, K.V., Delgado-Granados, H., Kent, A.J.R., 2008. Magmatic volatile contents and degassing-induced crystallization at Volcán Jorullo, Mexico: Implications for melt evolution and the plumbing systems of monogenetic volcanoes. Earth and Planetary Science Letters v. 269, p. 478-487.

Kahl, M., Chakraborty, S., Costa, F., Pompilio, M., 2011. Dynamic plumbing system beneath volcanoes revealed by kinetic modeling, and the connection to monitoring data: An example from Mt. Etna. Earth and Planetary Letters v.308, p.11-22.

Kahl, M., Chakraborty, S., Costa, F., Pompilio, M., Liuzzo, M. & Viccaro, M., 2013. Compositionally zoned crystals and real-time degassing data reveal changes in magma transfer dynamics during the 2006 summit eruptive episodes of Mt. Etna. Bulletin of Volcanology, v.75:692. doi:10.1007/s00445-013-0692-7

Lara, L., Lavenu, A., Cembrano, J., Rodríguez, C., 2006. Structural controls of volcanism in transversal chains: Resheared faults and neotectonics in the Cordón Caulle–Puyehue area (40.5°S), Southern Andes. Journal of Volcanology and Geothermal Research 158, 70-86.

Lasaga, A.C., Jiang, J., 1995. Thermal history of rocks: P-T-t paths from geospeedometry, petrologic data and inverse theory techniques. Journal of Science v. 295, p. 697-741.

Lees, J.M., Crosson, R.S., 1989. Tomographic inversion for three-dimensional velocity structure at Mount St. Helens using earthquake data. Journal of Geophysical Research, v. 94, p. 5716-5728.

Lohmar, S., Parada, M.A., Gutiérrez, F., Robin, C, Gerbe, M.C., 2012. Mineralogical and numerical approaches to establish the pre-eruptive conditions of the mafic Licán Ignimbrite, Villarrica Volcano (Chilean Southern Andes). Journal of Volcanology and Geothermal Research 235-236, 55-69.

López-Escobar , L., Parada, M.A., Hickey-Vargas, R., Frey, F.A., Kempton, P.D., Moreno, H., 1995a. Calbuco Volcano and minor eruptive centers distributed along the Liquiñe-Ofqui Fault Zone, Chile (41º-42º S): contrasting origin of andesitic and

basaltic magma in the Southern Volcanic Zone of the Andes. Contributions to Mineralogy and Petrology 119, 345-36.

López-Escobar, L., Cembrano, J., Moreno, H., 1995b. Geochemistry and tectonics of the Chilean Southern Andes basaltic quaternary volcanism (37–46°S). Revista Geológica de Chile 22 (2), 219–234.

Loucks, R., 1996. A precise olivine–augite Mg–Fe-exchange geothermometer. Contributions to Mineralogy and Petrology 125, 140–150.

Lüth, S., Wigger, P., 2003. A crustal model along 39°S from a seismic refraction profile. Andean Geology, v. 30 (1), 83-101.

Martin, V.M., Morgan, D.J., Jerram, D.A., Caddick, M.J., Prior, D.J., Davidson, J.P., 2008. Bang! Month-Scale Eruption Triggering at Santorini Volcano. Science, v. 321, p. 1178.

McGee, L.E., Beier, C., Smith, I.E.M., Turner, S., 2011. Dynamics of melting beneath a small-scale basaltic system: a U-Th–Ra study from Rangitoto Volcano, Auckland volcanic field, New Zealand. Contributions to Mineralogy and Petrology 162 (3), 547-563.

Menand, T., Annen, C., de Saint Blanquat, M., 2015. Rates of magma transfer in the crust: Insights into magma reservoir recharge and pluton growth. Geology v. 43, p. 199-202.

Moreno, H., Lara, L., 2008. Geología del área Pucón-Curarrehue, regiones de La Araucania y De Los Ríos. Servicio Nacional de Geología y Minería, Carta Geológica de Chile, Serie Geológica Básica. No. 115, Mapa Escala 1:100.000.

Morgado, E., Parada, M.A., Contreras, C., Castruccio, A., Gutiérrez, F., McGee, L., 2015. Contrasting records from mantle to surface of two nearby arc volcanic complexes: Caburgua-Huelemolle Small Eruptive Centers and Villarrica Volcano. Journal of Volcanology and Geothermal Research (submitted).

Morgan, D. J., Blake, S., 2006. Magmatic residence times of zoned phenocrysts: introduction and application of the binary element diffusion modelling (BEDM) technique. Contributions to Mineralogy Petrology, v.151, p.58-70.

Morgan, D.J., Blake, S., Rogers, N.W., DeVivo, B., Rolandi, G., Macdonald, R., Hawkesworth, C.J., 2004. Time scales of crystal residence and magma chamber volume from modeling of diffusion profiles in phenocrysts: Vesuvius 1944. Earth and Planetary Science Letters, v.222, p.933–946.

Németh, K., 2010. Monogenetic volcanic fields: Origin, sedimentary record, and relationship with polygenetic volcanism. In: Cañón-Tapia, E., Szakács, A., (Eds.), What is a volcano?: Geological Society of America Special Paper v. 470, p. 43-66.

Philibert, J., 1991. Atom Movements, Diffusion and Mass Transport in Solids, Les éditions de Physique, Les Ulis, France, p. 577.

Rutherford, M.J., 2008. Magma Ascent Rates. Reviews in Mineralogy & Geochemistry, v. 69, p. 241-271.

Rutherford, M.J., Hill, P.M., 1993. Magma ascent rates from amphibole breakdown: Experiments and the 1980-1986 Mount St. Helens eruptions. Journal of Geophysical Research, v.98, p.19667-19685.

Scandone, R.S., Malone, S., 1985. Magma supply, magma discharge and readjustment of the feeding system of Mount St. Helens during 1980. Journal of Volcanology and Geothermal Research, v.23, p.239-262.

Smith, I.E.M., Blake, S., Wilson, C.J.N., Houghton, B.F., 2008. Deep-seated fractionation during the rise of a small-volume basalt magma batch: Crater Hill, Auckland, New Zealand. Contributions to Mineralogy and Petrology v. 155, p. 511-527.

Sparks, R.S.J., Baker, L., Brown, R.J., Field, M., Schumacher, J., Stripp, G., Walters, A., 2006. Dynamical constraints on kimberlitic volcanism. Journal of Volcanology and Geothermal Research, v.155, p.18-48.

Spera, F.J., 1984. Carbon dioxide in petrogenesis III: role of volatiles in the ascent of alkaline magma with special reference to xenolith-bearing magmas. Contributions to Mineralogy and Petrology, v.88, p.217-232.

Zellmer, G.F., Blake, S., Vance, D., Hawkesworth, C., Turner, S., 1999. Plagioclase residence times at two island arc volcanoes (Kameni islands, Santorini and Soufriere, St. Vincent) determined by Sr diffusion systematics. Contributions to Mineralogy and Petrology, v.136, p.345–357.
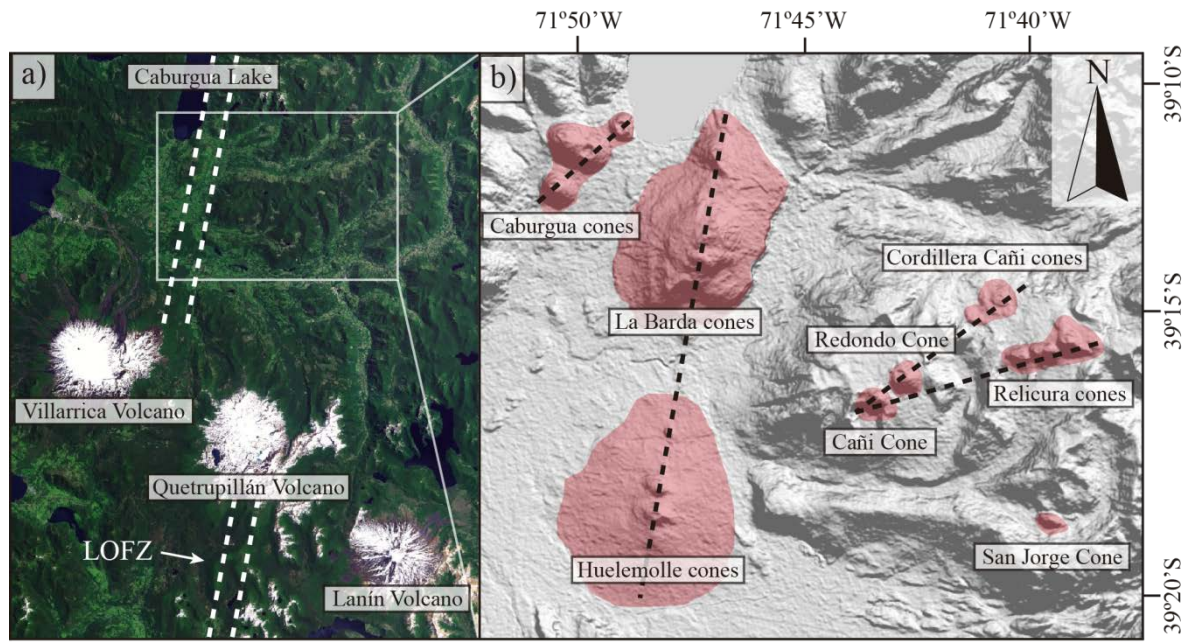
Figure 3.1. a) Geological context of the Caburgua cones. LOFZ: Liquiñe Ofqui Fault Zone (Cembrano et al., 1996) b) Local-scale distribution of the Caburgua cones and neighboring small eruptive centers. Dashed lines represent cone alignments that coincide with the LOFZ and associated NE-striking tension cracks (Cembrano and Lara, 2009).
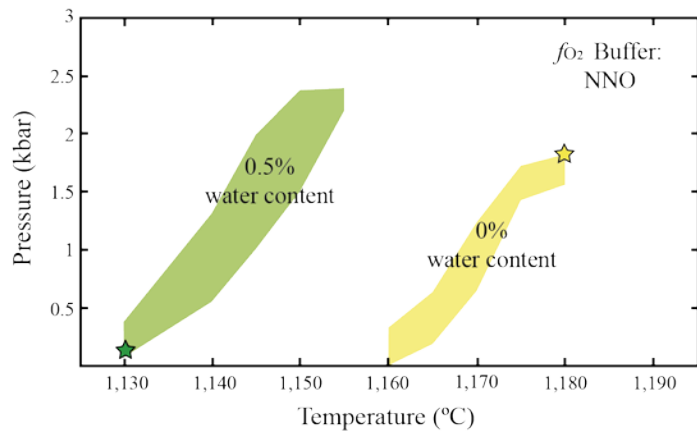
Figure 3.2. Stability P-T fields of olivine rim composition ($Fo_{77.5-78.5}$) at different water contents and under NNO buffer conditions. Yellow and green stars indicate the conditions for the calculation of the minimum and maximum time interval of olivine rim formation, respectively.
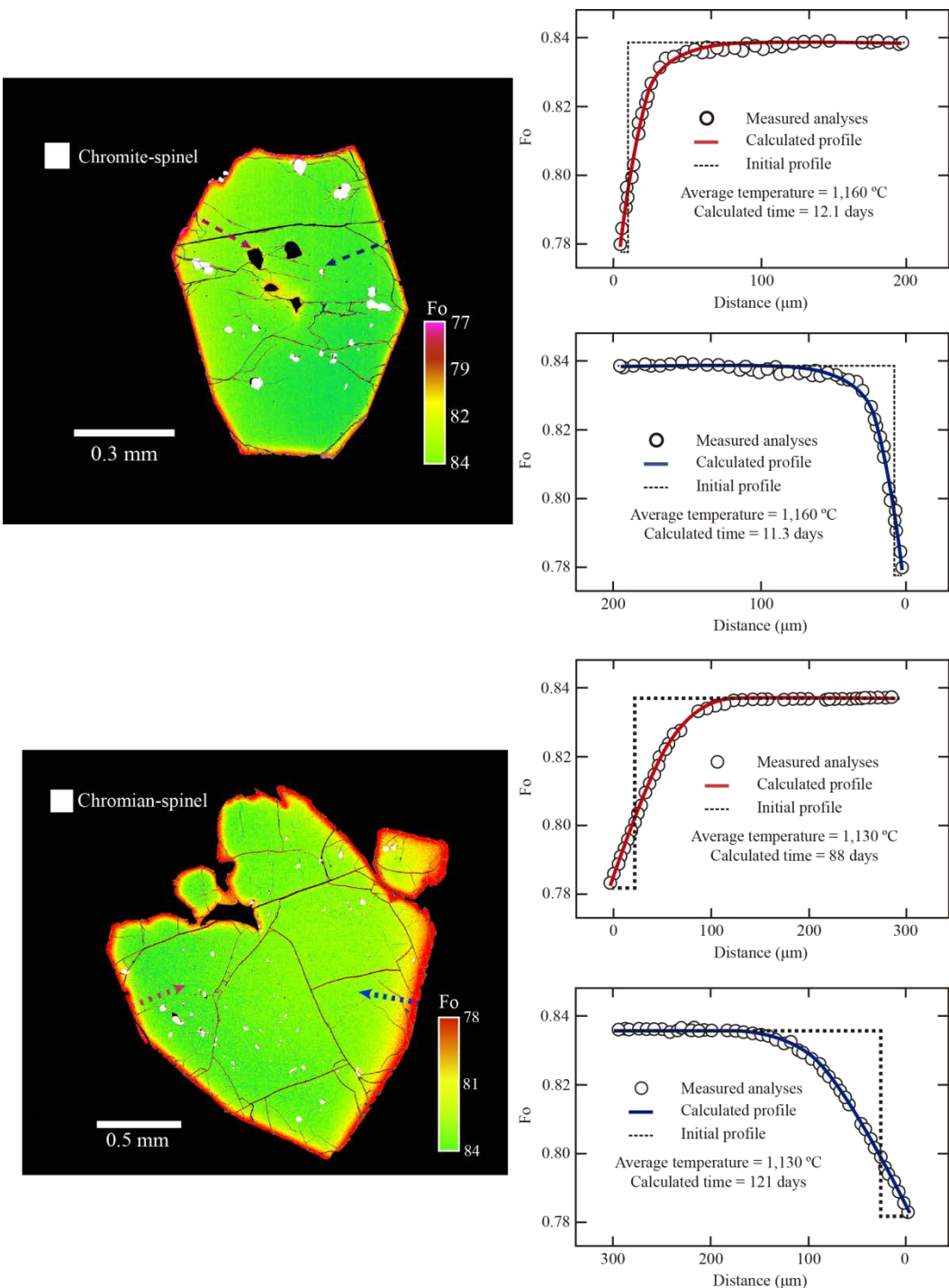
Figure 3.3. Example of olivine phenocryst profiles and the associated timescales. The figure a) shows the minimum calculated timescales, these are in the range between 11.3 and 12.1 days, whereas b) shows the maximum calculated timescales, these are in the range between 88 and 121 days. The considered average temperature was 1,160 ºC for minimum timescales, whereas the temperature for maximum timescales was 1,130 ºC. All calculated timescales are available in Table 1.
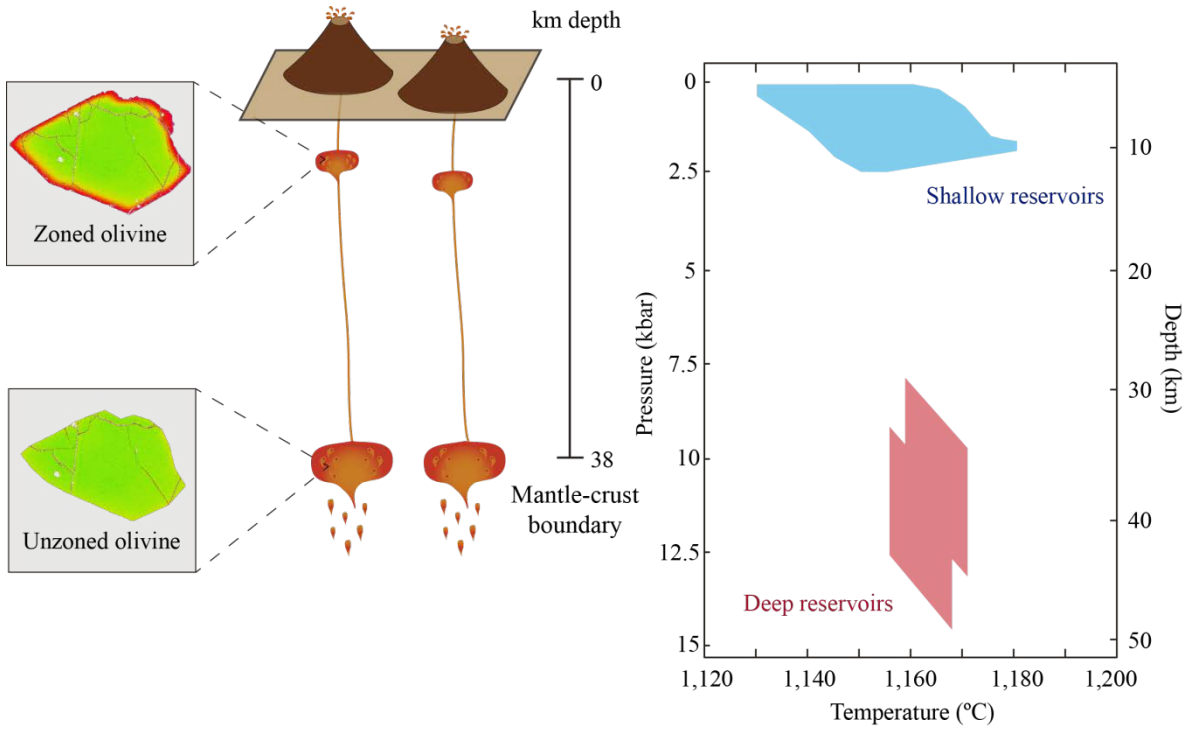
Figure 3.4. Schematic representation of the main characteristics of the reservoirs associated to Cabrugua cones. The studied volcanic complex would have at least one deep reservoir at the mantle-crust boundary and a transient shallow reservoir in the upper crust, where the magmatic residence time is short (< 121 days).

Table 1. Results of calculated times for olivine rim formation considering different conditions

Sample	Crystal number	Temperature (ºC)	Water content (%)	Pressure (kbar)	Buffer	Profile 1 (days)	Profile 2 (days)
CAB2-2	1	1,180	0	1.8	NNO	7.1	7.2
CAB2-2	1	1,160	-	0.9	NNO	11.3	12.1
CAB2-2	1	1,130	0.5	0.07	NNO	20	24.6
CAB2-2	2	1,180	0	1.8	NNO	28.3	40.8
CAB2-2	2	1,160	-	0.9	NNO	52	79
CAB2-2	2	1,130	0.5	0.07	NNO	88	121

CAPÍTULO 4

CONCLUSIONES

En la presente tesis se han estudiado los centros eruptivos menores Caburgua-Huelemolle (CHSEC) y el volcán Villarrica, en particular, la erupción de 1971. CHSEC y el volcán Villarrica son ejemplo de coexistencia de centros eruptivos menores y un estratovolcán; asociación común en la Zona Volcánica Sur de los Andes, Chile. Ambos complejos volcánicos son alimentados desde reservorios profundos con condiciones de presión y temperatura coincidentes con la profundidad del límite corteza-manto. Sin embargo, se reconocieron características importantes con respecto a su historia magmática pre-eruptiva en la corteza superior.

Los magmas de CHSEC habrían migrado desde el reservorio profundo hasta un reservorio transicional, en el cual habrían estado por tiempos menores a 121 días. Por otro lado, la lava de la erupción de 1971 del volcán Villarrica tuvo una historia más compleja, consistente con tasas mayores de alimentación de magma (bajas tasas de alimentación serían asociadas a volcanismo monogenético; Takada, 1994) y un reservorio intermedio a baja profundidad, donde los tiempos de residencia, consistentes con la homogenización del magma en la corteza superior serían del orden de décadas (35 años; Lohmar et al., 2012). Este reservorio fue sometido a un episodio de calentamiento previo a la erupción.

Los breves períodos de asimilación cortical son una razón por la cual, en términos generales, las lavas de los centros eruptivos menores son más máficas que

las de los estratovolcanes, que como en el caso del Villarrica, tienen un estado de estancamiento en la corteza superior.

La zona de falla Liquiñe-Ofqui, que controla la distribución de los CHSEC facilitaría el transporte de los magmas inicialmente estancados en la base de la corteza. Esta zona de falla permitiría que magmas de pequeño volumen, como los de los centros eruptivos menores, alcancen la superficie, sirviendo como una vía natural de ascenso.

Por otro lado, el volcán Villarrica está construido sobre una falla inactiva de basamento (Moreno y Clavero, 2006). Esto, adicionado a la presión ejercida por el edificio del volcán (Pinel y Jaupart, 2000), impedirían el ascenso de magma y facilitarían la construcción del reservorio somero.

Bibliografía

Hickey-Vargas, R., Moreno, H., López Escobar, L., Frey, F., 1989. Geochemical variations in Andean basaltic and silicic lavas from the Villarrica–Lanín volcanic chain (39.5°S): an evaluation of source heterogeneity, fractional crystallization and crustal assimilation. Contributions to Mineralogy and Petrology 103, 361–386. http://dx.doi.org/10.1007/BF00402922

Moreno, H., Clavero, J., 2006. Geología del volcán Villarrica, Regiones de La Araucanía y de Los Lagos. Servicio Nacional de Geología y Minería, Carta Geológica de Chile, erie Geología Básica, No. 98, Mapa escala 1:50000.

Lohmar, S., Parada, M.A., Gutiérrez, F., Robin, C, Gerbe, M.C., 2012. Mineralogical and numerical approaches to establish the pre-eruptive conditions of the mafic Licán Ignimbrite, Villarrica Volcano (Chilean Southern Andes). Journal of Volcanology and Geothermal Research 235-236, 55-69.

Pinel, V., Jaupart, C., 2000. The effect of edifice load on magma ascent beneath a volcano. In: Francis, P., Neuberg, J., Sparks, R.S. (Eds.), The Causes and Consequences of Eruptions of Andesite Volcanoes; Papers of a Discussion Meeting. Philosophical Transactions — Royal Society. Mathematical, Physical and Engineering Sciences 358, pp. 1515–1532.

Takada, A., 1994b. The influence of regional stress and magmatic input on styles of monogenetic and polygenetic volcanism. Journal of Geophysical Research 99, 13,563-13,573. http://dx.doi.org/10.1029/94JB00494